Review on the History, Research, and Applications of Electrohydrodynamics

Emmanouil D. Fylladitakis, Michael P. Theodoridis, and Antonios X. Moronis

***Abstract*— Corona discharge refers to the phenomenon when the electric field near a conductor is strong enough to ionize the dielectric surrounding it but not strong enough to cause an electrical breakdown or arcing between conductors or other components. This phenomenon is unwanted and dangerous in high-voltage systems; however, a controlled corona discharge may be used to ionize a fluid and induce motion by directly converting the electrical energy into kinetic energy. Phenomena that involve the direct conversion of electrical energy into kinetic energy are known as electrohydrodynamic (EHD) and have a variety of possible applications today. This paper contains a literature review of the research regarding the EHD effects associated with corona discharges, from the first observation of the phenomenon to the most recent advancements on its mathematical modeling, as well as the advancements on specific applications, such as thrust, heat transfer improvement, boundary layer enhancement, drying, fluid pumping, and cooling.**

***Index Terms*— Corona discharge, EHD-enhanced drying, electrohydrodynamics (EHD), electronics cooling, electrostatic fluid accelerator, finite-element method (FEM), micropump.**

I. Introduction

A. Brief History of the Electrohydrodynamic Effect—Early Years

The earliest observation and recording of electrohydrodynamic (EHD) effects have been made in 1629 by Niccolo Cabeo, who noticed that sawdust would be attracted toward an electrified body, touch it, and then be repelled [1]. Cabeo, however, was unable to realize that this behavior was due to an EHD effect; thus, the first official acknowledgement regarding the discovery of EHD has been given to Francis Hauksbee (1709), who recorded that he had experienced a weak wind blowing when holding a charge tube close to him. Hauksbee's work was continued by Newton [2], who baptized the phenomenon electric wind at the time, a name that lasted for centuries; however, nowadays, the term ionic wind is far more common. Wilson [3] had even been successful at making practical use of the electric wind as a driving mechanism of a rapid rotary pinwheel. However, even though EHD effects had been observed, the scientists simply lacked the knowledge and technology to fully explain it at the time. The first qualitative theory of the phenomenon is owed to Cavallo [4], who accurately described the electric wind while he was analyzing the motion of a fly.

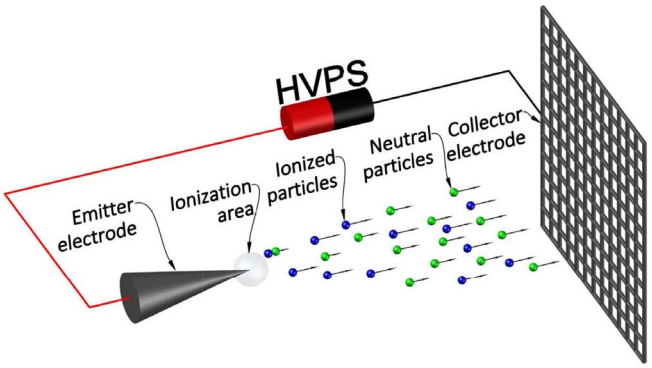

Fig. 1. Particle stream of a dc EHD device.

Significant progress was made several decades later, when Faraday [5] published his annotations on the electric wind. Faraday described the electric wind as a process of momentum transfer, caused by friction or collision between charged and uncharged gas particles, properly identifying the reason behind the movement of the air. Fig. 1 shows a basic graphic representation of the particle stream between two electrodes when high-dc voltage is applied to the emitter.

After 250 years from the first observation of EHD effects, Maxwell [6] performed the first qualitative analysis of the electric wind mechanism. Maxwell attached great importance to the study of the gaseous discharge despite his scarce knowledge in gaseous electronics, prophesizing that when such processes are better understood, they will throw great light on the nature of electricity, as well as on the nature of gases. Despite the fact that not even rudimentary mathematical treatment could be applied on theories regarding gaseous electronics at the time, Maxwell's work set the basis for future research as it was the most complete at the time and still preserves much of its validity even today.

B. Quantitative Research and the Befield–Brown Effect

Near the end of the 19th century, the very first quantitative analysis of the ionic wind was performed in [7].

Manuscript received August 13, 2013; revised November 13, 2013; accepted December 25, 2013. Date of publication December 27, 2013; date of current version February 6, 2014.

E. D. Fylladitakis and M. P. Theodoridis are with the Department of Electronics and Computer Engineering, Brunel University London UB8 3PH, U.K. (e-mail: emmanouil.fylladitakis@brunel.ac.uk; michael.theodoridis@brunel.ac.uk).

A. X. Moronis is with the Department of Energy Technology Engineering, Technical Educational Institute of Athens, Athens 12210, Greece (e-mail: amoronis@teiath.gr).

Color versions of one or more of the figures in this paper are available online at http://ieeexplore.ieee.org.

Digital Object Identifier 10.1109/TPS.2013.2297173

Chattock [7] derived an experimentally verifiable relationship between pressure and electric current for a configuration of parallel plane electrodes, setting the foothold for future research. Some years later, Peek [8] wrote one of the first books on high-voltage engineering focused on dielectric phenomena, titled Dielectric phenomena in high-voltage engineering. The book provided a wealth of information at the time, including the properties of gaseous, liquid, and solid insulations, methods useful for designing devices, transmission lines, high-voltage parts and equipment, as well as methods to perform high-voltage engineering experiments, measurement of high voltages, field sketching, and explanations of various dielectric phenomena and experimental data. In his book, Peek provided vast information on corona-related effects and mechanisms, which were of critical importance to future researchers.

Significant importance has also been given to the work of Thomas Townsend Brown, who noticed that net mechanical force was exerted from a Coolidge X-Ray tube when its asymmetrical electrodes were connected to a high-voltage power source. Brown collaborated with Paul Alfred Biefeld and they published an article describing their findings in 1929, indicating that this was not due to an X-ray effect but due to the ionized particles created by the high-voltage electrode, which later came to carry the names of the scientists and become known as the Biefeld–Brown effect [9]. Despite their extensive work on the subject, there have been no scientific publications or books regarding their research, aside from some patents. In addition, by reviewing the article and some of their first patents, it would appear that Brown initially misinterpreted the phenomenon for an antigravity effect that, among other parts of their work, has been scientifically disproved [10].

Interest in EHD phenomena resurged several years later, when Lob [11] investigated Chattock's study of the ionic wind and extended it to other geometries. The thrust properties of the phenomenon also became of interest to the military and Lob's work was soon enhanced by United States Air Force (USAF) Captain Harney [12]. Harney examined the electrical parameters of a corona discharge and the variations of particular aerodynamic parameters. Both Lob's [11] and Harney's [12] works have been summarized and expanded by Otmar Stuetzer [13], whose publications were the most complete to that time.

C. Governing Equations and the Mathematical Problem

The corona discharge in fluids is a complex physical phenomenon which is not yet fully understood. Nevertheless, the simplification of the mathematical problem is conceivable when appropriate boundary conditions are set [14]. Poisson's equation describing the electric potential V (1) may be combined with Gauss's law describing the electric field intensity $\boldsymbol{E}$

$$\nabla^2 V = -\frac{\rho}{\varepsilon_o} \tag{1}$$

$$\boldsymbol{E} = -\nabla V \tag{2}$$

where ρ is the space charge density, ε_o is the dielectric permittivity of the fluid, and V is the voltage potential of the emitter electrode.

Considering the current continuity condition, the current density j may be described by

$$\nabla \cdot \boldsymbol{j} = 0. \tag{3}$$

Current density $\boldsymbol{j}$ is derived from the combination of three parameters: 1) the ions moving due to the electric field; 2) the charges transported via the molecules due to the fluid flow; and 3) due to diffusion. Therefore, current density may be also described by

$$\boldsymbol{j} = (\mu_\varepsilon \rho \boldsymbol{E} + \rho \boldsymbol{U} - D\nabla\rho) \tag{4}$$

where μ_ε is the ion mobility, D is the ion diffusion coefficient, and $\boldsymbol{U}$ is the velocity of the fluid flow.

The Navier–Stokes equation (5) describes the motion of the fluid

$$\rho \cdot \left[\frac{\partial \boldsymbol{U}}{\partial t} + (\boldsymbol{U} \cdot \nabla)\boldsymbol{U}\right] = -\nabla\rho + \mu\nabla^2\boldsymbol{U} - \rho\nabla V \tag{5}$$

where ρ is the density of the fluid, p is the pressure, and μ is the dynamic viscosity of the fluid.

If the fluid flow is incompressible and the density is constant, then the continuity equation reduces to

$$(\nabla \cdot \boldsymbol{U} = 0.) \tag{6}$$

Therefore, these equations can now be used, subjected to proper boundary conditions, to present a feasible solution of the mathematical problem. However, for any geometry where the voltage V is a function of two or more coordinates, the mathematics for solving the described problem may become quite complicated [14]. Therefore, the development and use of numerical techniques were necessary for the calculation of the aforementioned electrical figures, which significantly impaired the advancement of EHD-related research at the time. Thus, the research interest in EHD resurged only recently, after the explosive development of computers, as the known numerical methods require high computing power.

II. Advances on the Modeling of the EHD Phenomenon

As soon as it became clear that a mathematical breakthrough would be necessary for the solution of the aforementioned equations, several engineers and scientists explored other methods to calculate electric field-related phenomena. The finite-element method (FEM) was being established roughly at the same time as the resurgence of the interest in EHD and scientists soon realized that it could lead to satisfactory results via relatively simple calculations [15], [16]. Simply put, FEM divides the domain of the unsolvable problem into numerous triangular elements, forming a mesh of minute subdomains, which subdomains can then be individually solved through consecutive partial differential equations and lead to an approximate solution. This mesh can be denser where finer accuracy is required and sparser in other areas. However,

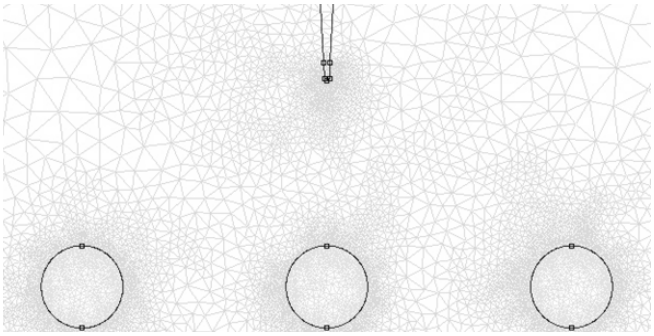

Fig. 2. Detail of the elements mesh from a modern FEM simulation software (circular collector electrode radius = 1 mm) [19].

this method leads to massive algebraic systems once high accuracy is vital, even in very small systems, especially if the radii of the electrodes are very small.

Early attempts to use the FEM to compute the electrical figures of a corona discharge inside a minute, simple region has been made and the problem proved to be quite complex, even though only a quarter of it required an actual solution due to symmetry [17]. The computation of even basic geometries required immense processing power, which was not available at the time. The accuracy of such simulations was low and using the FEM for the calculation of complex configurations and or configurations using electrodes with very small curvatures remained a prohibitively time consuming procedure. Even several years later, FEM studies on corona discharges were being performed with a mesh formed by a few hundred elements and the computers available at the time would need about an hour to perform a 2-D simulation of a simple geometry [18]. In terms of comparison, modern computers can generate the mesh of a 2-D problem with hundreds of thousands of elements and solve it within a few minutes. Fig. 2 shows a detail of a mesh as it has been calculated by a modern simulation software.

As the processing power of computers increased, several scientists began the development of more sophisticated algorithms to simulate complex electric fields in space, as well as flows generated by corona discharges. The first complete algorithm was developed by Morrow [20], who managed to analyze all of the major processes of the corona discharge in the time domain. Several improved algorithms were presented in the following years [21]–[23]; however, their common characteristic was the significant complexity and the requirement for high computing power. Most of these numerical models use a hybrid combination of multiple numerical methods, such as the boundary element method, the method of characteristics, the finite-difference and finite-volume methods, as well as the FEM.

There have also been numerical models developed via the application of commercial computational fluid dynamics (CFD) software [24]–[27]. Nevertheless, FEM simulations display much higher popularity as they have been proven to be the most widely accepted computational method for the modeling of electromagnetic problems [28], [29]. Although both open and commercial software, utilizing the FEM to model electrostatic problems has been available since the dawn of the 21st century [30], [31], the modeling of corona discharges and EHD flows met an explosive growth after 2007, due to the high processing required to reach fine spatial discretization, especially when electrodes with curvatures of very small radii are involved. Studies and models of basic geometries, such as wire-to-wire [32], cylinder-to-wire-to-plane [33], wire-to-cylinder [34], and needle-to-plane [35], can be found in bibliography published during the past few years. However, most of the research concerning the ionic wind and EHD in general, is performed to evaluate specific practical applications rather than finding a universal solution.

III. Thrust

Ever since the discovery of the Befield–Brown effect, a major part of the research regarding the phenomenon was focused almost entirely on thrust applications. Thomas Townsend Brown had filed several patents of apparatuses intended to be used as propulsion motors, based on his discoveries [36]–[38]; however, the patent filed by Seversky [39] during the same period, baptized the vehicles propelled by EHD thrusters as Ionocrafts, clearly in an effort to differentiate his work from that of Townsend Brown and is likely much to blame for today's terms of ion thruster and ionic wind. A few years later, Christenson and Moller [40] published a paper with a basic experimental investigation of a multiple needle-to-plane EHD thruster, which reached an electric to kinetic energy conversion efficiency of approximately 1%. Today, 40 mm × 40 mm × 20 mm and 60 mm × 60 mm × 20 mm electric fans have an electric to kinetic energy conversion efficiency of about 0.55% [41] and 0.62% [42], respectively. Still, the thrust levels of Christenson's experiments were disheartening for the size and weight of the apparatus.

Because of the complexity of the EHD phenomena that make it difficult to reach analytical solutions, especially in complex geometries, research on atmosphere-based EHD thrusters has nearly been abandoned. Military research has been taking place from the USAF and the SAF, which led to the advancements on space thrusters during the cold war, with the most notable achievement being the Hall Effect thrusters, which the Soviets have been using to stabilize their satellites for decades [43]. Several EHD and electromagneto-hydrodynamic (EMHD) designs have been developed since then for spacecraft propulsion but the involvement of the military withheld most of the scientific publications until after the dissolution of the USSR [44]–[47]. Such designs require the presence of a gaseous or liquid propellant, usually xenon gas due to its low ionization potential and heavy molecular weight and, despite the very low levels of thrust, EHD and EMHD space thrusters achieve much higher values of specific impulse over chemical rockets and are today considered to be the only viable solution for long-term space travel.

Due to their very weak thrust and with no foreseeable technological breakthrough in sight, very few researchers even tried to assess the performance of EHD thrusters for applications in the atmosphere of earth. As the understanding of the phenomenon grew in the past decade, researchers began

by disproving the claims that the Biefeld–Brown effect is an antigravity effect and fully explained it through the simple theory that the EHD effect uses only electrostatic forces and the transfer of momentum by multiple collisions with the air molecules [10], [48]. Research followed on the Ionocraft [49], with researchers modeling the gas flow of the levitation apparatus, experimentally modeling the electrical and physical characteristics of the flyers [50], [51], as well as trying to optimize the design via the use of the latest FEM modeling software [52].

Aside from the research centered on the triangular lifter apparatus first designed by Townsend Brown, a few researchers have tried to develop new methods and EHD thruster electrode geometries. However, the applicability of EHD thrusters in nonconductive liquid environments has been validated through the presentation of a functional microboat, propelled by a basic EHD microthruster [53]. An alteration of the original levitation device was also presented in the form of an indoor surveillance blimp, where helium balloons keep the apparatus afloat without the need of any other levitation force and the EHD device is solely used as a thruster [54]. Although the concept was interesting, the overall size of the apparatus makes practical applications appearing unrealistic, as the balloons were about 1.5-m long and over 1-m wide for an EHD thruster of 106 gr to levitate. A relatively simple, 1-D model of ideal EHD thrusters has also been recently presented in [55], shedding some light on the calculations of the thrust and efficiency of EHD lifters, as well as their principal performance limits.

Despite the slow progress of research on atmospheric EHD thrusters, a thorough article was recently released by NASA on ionic wind propulsion, which explored both the same wire to fins geometry as the lifter designed by Townsend Brown and a needle-to-fins electrode design [56]. The scientists performed parametric experiments to compare the two geometries, optimize the number, distance and size of the electrodes, model the electrical characteristics of the thrusters, and derive mathematical relationships for the optimized designs. Although the authors claimed that the EHD thrusters in their current form did not appear to have any practical use, significant progress was made and they made several research suggestions, which inspired further research.

A recent study experimentally explored the potential of wire-to-cylinder EHD thrusters, as well as the performance of dual-stage three-electrode wire-to-rod-to-cylinder EHD thrusters (Fig. 3), which, however, did not meet the expected results as, according to the author, very high voltage was necessary to generate thrust between the intermediate and the collector electrode and also a reverse corona was being formed at the intermediate cylinder electrode [57].

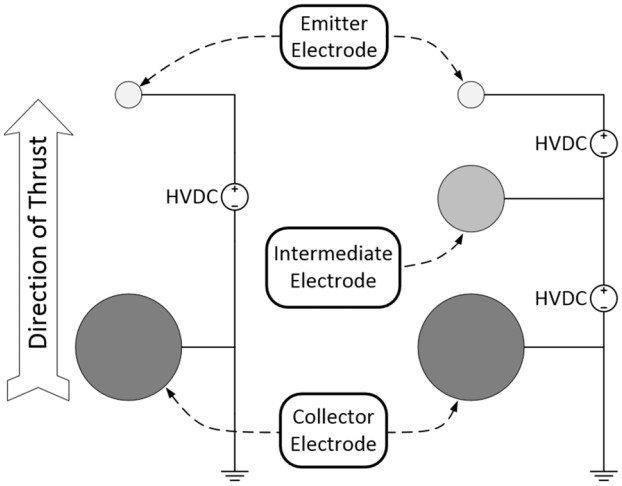

Fig. 3. Wire-to-cylinder single stage (left) and wire-to-rod-to-cylinder dual stage (right) EHD thruster designs explored by the MIT [57].

IV. Flow and Heat Transfer Enhancement

Research on the effects that EHD flow would have on the boundary layer of a fluid flow and on heat transfer via convection began at roughly the same time as the research on EHD thrust engines [58]. For the following years, significant research took place regarding the alteration of the boundary layer using corona discharges, thus improving forced convection heat transfer or reducing drag; however, most such research was focused on improving existing heat exchangers and known geometries rather than creating standalone ionic wind pumps, which would not require externally forced flow.

Due to the complexity of the EHD phenomena, research progress initially was very slow. Fernandez was first to validate that EHD could bring a significant improvement to forced convection inside tubes [59]. Thorough experimental testing of his work and validation of his finding came many years later [60], suggesting that the heat transfer rate could increase up to 20 times over using a concentrical wire-to-cylinder configuration, even though the pressure drop increase would only triple. Experiments for the same geometry have also been performed in [61], which concluded that the maximum possible heat transfer enhancement was 215% for a single emitter electrode and 260% if two emitter electrodes were used; however, that enhancement would diminish as the Reynolds number increased. A recent study of the same configuration displayed that the heat transfer enhancement can reach up to 870% over natural flow [62]. The plane-to-wire-to-plane configuration was also explored a few years later, with the researchers' experiments displaying that a heat transfer enhancement of up to 600% is possible in rectangular channels, although the enhancement once again diminished at high Reynolds numbers [63]. Another research exchanged the flat plane for a wavy one and used multiple emitters, creating a multiwire to wavy plane electrode configuration, which reached a performance enhancement ratio of 6:1 for low Reynolds numbers but, once again, the enhancement ratio fell below 2:1 for $\mathrm{Re} \geq 500$ [64].

Significant research has been performed in [65]–[67] on the effect of a corona discharge on the boundary layer when bulk flow already exists, using a wire-to-plate electrode configuration, with several papers published on the subject. The research displayed that there is a significant enhancement on the bulk flow velocity within the boundary layer for velocities up to 25 m/s, the ratio of which, however, decreases as the bulk flow velocity increases. Additional research on the

TABLE I
EHD-AUGMENTED HEAT TRANSFER RESEARCH RESULTS

Author(s)	Electrode geometry	Working medium	Heat transfer coefficient improvement
Robinson [69]	Platinum wire	Air	320%
Mizushima et al. [70]	Coaxial wire-to-tube	Air	150% (Re=2000) 300% (Re=700)
Velkoff and Godfrey [71]	Wire-to-plate	Air	≈250%
Tada et al. [72]	Plate-to-plate	Air	270%
Nelson et al. [73]	Coaxial wire-to-tube	Air	260%
Velkoff [76]	Coaxial wire-to-tube	Air, Nitrogen	100% (Re=3000)
Moss and Grey [75]	Coaxial wire-to-tube	Nitrogen	35% (Re=1200)
Grosu and Bologa [77]	Coaxial wire-to-tube	Air Helium Carbon dioxide Argon	200% (Air) 200% (He, 21 atm) 400% (CO2) 150% (Ar, 1.4 atm)
Choi [78]	Coaxial wire-to-tube	R113	100%
Seth and Lee [79]	Coaxial wire-to-cylinder	R113	60%
Holmes and Chapman [80]	Plate-to-plate (wedge)	R114	Up to 900%
Damianidis et al. [81]	Tube-to-plate	R114	8%
Karayiannis T.G. [82]	Rod-to-tube	R11 R123	≈0% (R11) 830% (R123)
Feng and Seyed-Yagoobi [84]	Coaxial wire-to-tube	R134a	≈100%

same configuration has been carried out in [68], exploring the enhancement of external forced convection on a heated flat plate. Their experiments displayed that, for a bulk flow velocity of less than 1 m/s, the thermal performance enhancement was over 200%.

Scientists also explored the viability of using EHD to enhance the performance of widespread heat transfer applications. Significant research took place on the augmentation of the heat transfer coefficient in existing systems, which were using air as the cooling medium. Early research results were aligned, with the heat transfer coefficient being augmented by 250%–320% [69]–[73]. However, [70] noticed that the augmentation would diminish as the Reynolds number increased, dropping to 150% for Re = 2000 and there was a little effect once the Reynolds number would be over 4000. Based on these results, [74] proposed that the exploitation of EHD could enhance the efficiency of building Heating, ventilation and air conditioning systems, displaying impressive performance increase potential and possibly reducing the heat exchange area enough to make use of renewable energy sources, the use of which was cost inhibitive due to the excessively large exchangers required. Aside from air, scientists also examined the heat transfer enhancement that EHD could offer to other cooling mediums. Early research was mostly based on gaseous heat transfer media, such as nitrogen [75], [76], argon, carbon dioxide, and helium [77].

More recent research, however, has been mostly based on phase-changing fluids. The performance augmentation of systems using R113 has been explored first [78], [79], with researchers reporting an enhancement between 60% and 100%. A similar research claimed that the performance of a system using flat silver-plated electrodes and implementing R114 may be increased up to tenfold [80]. Nevertheless, future research on system using R114 as the heat transfer medium displayed performance enhancements as low as 8% [81]. An experimental research using a multiple wire-to-cylinder EHD apparatus and with R123 and R11 as the heat transfer medium has been performed, indicating that the fluid properties are critical to the EHD enhancement ratio, as there was an enhancement of over nine times with R123 but negligible enhancement while using R11 [82]. The nowadays popular refrigerant R134a has also been examined with the use of a concentrical wire-to-cylinder electrode configuration. The first experiments were made with a steady high voltage applied to the emitter electrode [83] and a numerical analysis followed afterward [84], both displaying that the augmentation of the heat transfer coefficient is significant when R134a is used but the pressure drop penalty was too great for the technology to become an industrially viable application. Recently, experiments were also performed with the same concentrical wire-to-cylinder geometry by applying a pulsating high voltage to the emitter electrode [85], displaying that the use of pulsed voltage can widen the range of heat transfer and pressure drop, making the systems more amenable to control through the frequency of the pulsations. Table I summarizes the research results on EHD-augmented heat transfer to this date.

Finally, there has also been significant research regarding the EHD flow, which develops in electrostatic precipitators (ESPs). EHD flow in ESPs is a byproduct of their intended purpose, which is to induce an electrostatic charge on the particles of a flowing fluid, creating electrostatic attraction that will force them to move toward a grounded collector, thus effectively removing them from the stream. This flow of charged particles, however, alongside the ionization of particles of the fluid itself, creates an EHD flow that may have a detrimental effect on the performance of the precipitator at low bulk fluid speeds, or is inconsequential at higher bulk fluid flow speeds [86], [87]. Niewulis *et al*. [88] also hypothesized that the EHD flow affects the collection efficiency of ESP, with the effect being greater as the size of

the particles decreases. There have been numerous studies, both simulated and experimental, toward the evaluation of EHD flows inside ESPs of various electrode configurations [89]–[92]. Despite the degrading effect that EHD flow may have on the performance of ESPs, however, recent studies showed that the ozone generation of the corona discharge in air can act as a catalyst, incinerating unwanted particulates in the gas flow [93], [94].

V. Drying and Evaporation

During experiments regarding the lethality of ions on microorganisms, [95] discovered that the presence of ions in clean air increases the evaporation rate in droplets. Three decades later, Barthakur, who was observing the progress on the enhancement that ionic wind can offer to heat transfer, investigated the influence that the presence of positive and negative ions could have on evaporation rates. Early studies displayed very promising results, significantly increasing the evaporation rates of thin layers of liquids [96], saline water [97], and soil samples [98]. Soon afterward, it was also discovered that the ionic wind could significantly enhance the dehydration rates of potato slabs, which drew the attention of the agricultural and energy industries [99].

Over the past couple of decades, significant research has been performed over the enhancement of the evaporation rates that EHD could offer. Many researchers focused on the effect that the phenomenon would have on water [100]–[102]. Their results on the simplicity and efficiency of EHD drying have led to many researchers exploring the viability of EHD drying for specific industrial applications. As the most effective drying method in the food industry was the energy-hogging use of ovens and energy prices were continuously rising, there was a great interest in exploring new more efficient drying methods. After a team of scientists proved that EHD drying can be very effective for drying apple slices and offer great advantages over heat-based methods [103] and, in conjunction with the research on the water evaporation rates, there has been an explosion of articles exploring the effect of EHD drying on a variety of nutrients [104]–[110]. Each and every one of these studies concluded that the quality of the product, in terms of color and appearance, has been greatly increased, in addition to their nutrient value due to the sustainment of vitamins and other high-value ingredients, which are usually destroyed by heat-based drying techniques. It has also been proved that EHD drying is a far more energy-efficient method than any form of thermal drying and, in conjunction with the higher end-product quality due to the nonthermal drying process, is highly valuable to the food industry [107]. Research has also been performed on the EHD drying of nonedible materials, such as Agar Gel [111]. The energy industry began displaying great interest as well, as it was proved that EHD drying can enhance the quality of rapeseed [112], commonly used for the production of biofuels, for a considerably lower energy cost than heat-based drying methods, which could lead to less expensive and higher quality biofuels.

The research by the food industry has also brought about results regarding the performance of various electrode configurations. In 2002, the feasibility of a single wire emitter electrode design has been evaluated and displayed that significant drying performance enhancements can be had even by this very simple electrode geometry [113]. A few years later, the same research team also published a paper on the performance of a drying apparatus using multiple needle emitters, the performance of which, however, appeared inferior to that of the single-wire emitter [114]. Another experimental study has been performed by another research team with a multiple needle-to-plate electrode configuration, which displayed excellent performance, even though it was not apparent that there has been any optimization regarding the geometry of the electrodes [115]. A drying apparatus using a wire-to-plate electrode configuration has also been experimentally tested, with the research team displaying that the fabrication of an entire functional drying system is fairly easy and can effortlessly be scaled to industrial applications [116]. Table II summarizes the research results on EHD-augmented drying to this date.

VI. Fluid Pumps

A. General Research on EHD Fluid Pumps

The first to suggest the possibility of designing a functional electrostatic blower (i.e., an EHD pump) were Robinson [117] and Stuetzer [118], during their research on the ionic wind. Both researchers examined the same geometry and, therefore, their conclusions were very similar. By experimentally testing a needle-to-ring electrode geometry, Robinson evaluated the conversion efficiency from electrical energy to mechanical energy via corona discharges but was disheartened by the mediocre results of his experiments, which displayed an efficiency of less than 1%; he did, however, explicitly mention that EHD pumps have several advantages over mechanical pumps, the main being the lack of moving parts, as a result of which there are no vibrations, no wear and tear, no lubrication requirements, and no gyroscopic or rotational effects, as well as virtually no sound during operation.

The low electrical to mechanical energy conversion efficiency is one of the largest problems of EHD pumps and a few steps have been taken toward its improvement, yet there have been a few experimental studies focused on improving the exit fluid velocity and efficiency of EHD pumps. However, we should note that due to the different equipment and methods that each researcher used to measure the fluid speed and calculate the efficiency of the experimental device, the results of these studies are not directly comparable with each other.

Important work toward this end has been performed in [119], which focused on improving the electrical to mechanical energy conversion efficiency of the needle-to-ring and needle-to-mesh electrode configurations. Furthermore, the researchers tested both positive and negative corona discharges, which occur when positive and negative high-voltage potential is applied to the emitter electrode, respectively, and their effect on various mesh configurations. It was determined that positive coronas are generally capable of producing higher air velocities, reaching a maximum air velocity of 8 m/s with a positive corona discharge, while a negative corona discharge would generate a maximum air velocity of 5 m/s.

TABLE II
EHD-ASSISTED DRYING ENHANCEMENT RESEARCH RESULTS

Author(s)	Electrode geometry	Drying material	Evaporation rate improvement over ambient air drying
Barthakur and Arnold [100]	Needle-to-Plane	Water	≈300%
Lai et al. [101, 114]	Needle-to-plane	Water	Up to 126%
Lai et al. [101, 113]	Wire-to-plane	Water	Up to 240%
Alem-Rajabif and Lai [102]	Wire-to-plane	Water	Up to 270%
Barthakur and Bhartendu [96]	Needle-to-Plane	Water (100ml)	≈400% max
		Ethyl alcohol (100ml)	≈250% max
		Carbon tetrachloride (100ml)	≈350% max
N.N Barthakur [97]	Needle-to-Plane	Saline water	210 to 270% (depending on NaCl % concentration)
Barthakur and AL-Kanani [98]	Needle-to-Plane	Moisture (soil samples)	200% to 535% (depending on soil composition)
Chen and Barthakur [99]	Needle-to-Plane		200% (15 min)
		Potato slabs	170% (45 min)
			140% (180 min)
Hashinaga et al. [103]	Needles-to-plane	Apple slices	Up to 120%
Bajgai and Hashinaga [104]	Needles-to-plane	Spinach	Up to 300%
Cao et al. [105]	Needles-to-plane	Wheat	50% at 50 °C, 60% at 35 °C, 90% at 20 °C
Li et al. [106]	Needle-to-plane	Okara cake	Up to 220%
Bajgai and Hashinaga [108]	Needles-to-plane	Radish	Up to 470%
Esehaghbeygi and Basiry [109]	Needles-to-plane	Tomato slices	Up to 100%
Alemrajabi et al. [110]	Needles-to-plane	Carrot slices	Up to 420%
Goodenough et al. [107]	Wire-to-plane	Biscuits	Up to 450%
Bai et al. [115]	Needles-to-plane	Scallops	617%
Basiry and Esehaghbeygi [112]	Needles-to-plane	Rapeseed	Up to 275%
Isobe et al. [111]	Needle-to-plane	Agar gel	Up to 230%

The researchers also determined that the air velocity and uniformity are being aided by a dense grid of thin collector electrodes. Regarding the electrical to mechanical energy conversion efficiency, the study clearly displayed that mesh collector electrode configurations are superior to ring collector electrodes, plus that positive coronas are more efficient than negative ones. The optimal configuration generated an air velocity of 8 m/s with an efficiency of 1.72%, more than double the efficiency recorded in early studies of EHD phenomena. The higher efficiency of the positive coronas for EHD air pumps has also been verified in [120], which experimentally tested the static efficiency of a similar five needle-to-mesh EHD pump prototype. The researcher found that the static efficiency of a positive corona may reach up to 14%, while the maximum static efficiency of a negative corona is less than 2%.

Moon *et al.* [121] later presented a more complex needle-to-mesh EHD pump, with the emitter electrode surrounded by a ring at the same voltage potential. With this design, the research team claims to have improved the electrical to mechanical conversion efficiency of EHD pump by 2.5 times compared with the needle-to-mesh electrode design, yet the efficiency of the conversion was parallel to that of the optimized needle-to-mesh design presented in [119].

Recently, a study once again investigated the conversion efficiency of the needle-to-grid geometry EHD pump (Fig. 4), extending the research to a cascading design and for up to six consecutive stages [122]. Through a parametric study, the research team derived that the wind speed is a linear function

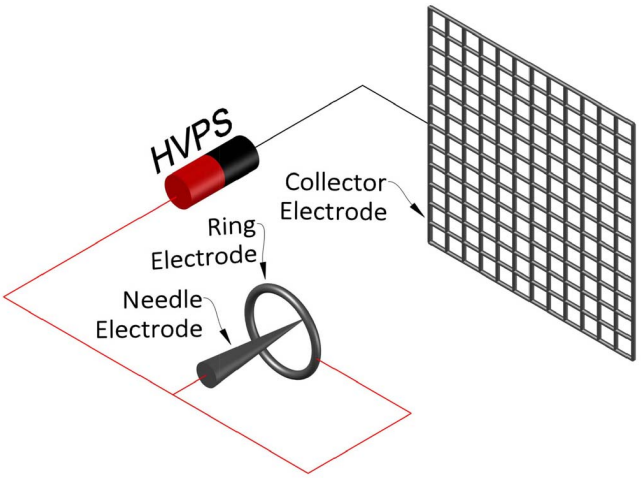

Fig. 4. Schematic view of the needle/ring to mesh experimental setup [121].

of the voltage applied to the emitter, as well as a function of the square root of the current multiplied with an empirical constant.

As the efficiency of EHD pumps is proportional to the velocity of any existing bulk flow [123], it was also shown that cascading EHD pumps increase not only the exit wind velocity of the EHD pump but the overall efficiency of the device as well. Noteworthy research on needle-based emitter electrode configurations has been performed in [124], which experimentally tested the performance of multiple EHD pump

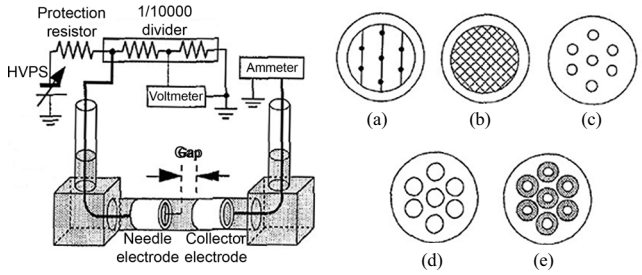

Fig. 5. Experimental configuration and the summary of electrode configurations used to assess the needle emitter-based EHD pumps [124]. (a) Needle electrode. (b) Collector (mesh). (c) Collector (3 mm holes). (d) Collector (6 mm holes). (e) Collector (tapered holes).

geometries using needles as the emitter electrodes and several different collector electrodes (Fig. 5). The study gave very useful conclusions regarding the dependence of air pressure to the applied voltage and concluded that the radius of the needle is a vital factor for the overall performance of the EHD pump. Strangely, however, the authors mentioned that there was no pressure creation with positive polarity during their experiments, while later research proved that not only the positive corona is capable of producing flow but it is more efficient as well, even with a similar needle-to-mesh electrode configuration [119].

A later study, assessing the effect of the voltage on the wind velocity using a needle-to-ring electrode configuration, displayed that the EHD pump operated properly with positive voltage applied to the emitter, reaching exit air velocities in excess of 2 m/s [125]. Future research by the same author offered further optimization of the design, which enhanced the performance of the EHD pump by implanting the collector electrode to the tube walls and also explored the performance of a cascading design for up to seven stages [126]. The design was further enhanced by the change of the simple needle electrode to a wet porous point electrode, which the author experimentally tested to be 95% more efficient for positive corona discharges and 30% more efficient for negative and ac corona discharges [127]. Another study has been performed to analyze the ionic wind velocity of a needle-to-cylinder electrode EHD gas pump [128]. However, although the study included very detailed results on the experimental design's performance and efficiency, neither the experimental setup appeared to be optimized nor any useful data on how to optimize such an electrode configuration have been disclosed. The effect of the number of stages of a multiple needle-to-mesh EHD pump prototype on the performance of the device has also been recently examined, indicating that an average flow velocity of 7.39 m/s is possible from a 20-mm-wide experimental device with a five-stage cascading configuration [129]. However, the authors also indicated that the efficiency of the design decreased as the number of stages increases [130], which is in complete contradiction with the findings of previous researchers [122]. Despite that the needle-to-mesh electrode configuration remained by far the most popular for years, during the past decade, researchers also began exploring EHD pumps based on different electrode configurations. A mathematical model for the needle-to-plate EHD air pump has been developed, verified by a parallel experimental study using a needle-to-mesh EHD air pump, reaching an exit air velocity of 4 m/s with an applied voltage of 13 kV and suggesting that the results are similar when using either a plate or a dense mesh as a collector electrode [131]. Further experimentation with laser-induced phosphorescence velocimetry revealed the profile of the ionic wind velocity of the needle-to-plate electrode configuration, which reached 20 m/s near the tip of the emitter electrode when the applied voltage was 10 kV [132].

A following publication, describing a multiple needle-to-mesh EHD pump, demonstrated that an anode voltage of higher than 26.5 kV for a 2.5-cm gap and higher than 29 kV for a 3.0-cm gap was required for the wind velocity to reach a measurable value [133]. In this particular study, however, no information was given regarding the energy conversion efficiency of the apparatus, electrode current, mesh size, precise electrode curvatures, or even the detailed number of needles, which create the emitter electrode. Apparently, the configuration was far from optimized, generating an electric field too uniform for the generation of a workable air flow, as no electrorheological effects are observed in uniform electric fields [134]. The effect of the number of emitter electrodes on the performance of the EHD pump has been studied some years later [135], with the author seeking to optimize the number of electrodes within a rectangular flow duct but without offering a universal solution.

A plate-to-plate configuration has also been explored via an experimental design, with the apparatus reaching speeds of nearly 1 m/s at the end of the 170-mm-long and 25-mm-wide collector electrode [136]. Although the positive corona discharges were becoming more and more popular, a study of the negative corona discharge with a wire-to-cylinder EHD pump has also been presented and focused on the power consumption of the experimental setup; however, the conversion efficiency was very low, at about 0.138% for an approximate average exit wind speed of 1.4 m/s [137].

Even though most of the researchers have been investigating the performance of positive corona discharge EHD pumps, a study of the efficiency that a wire-to-cylinder EHD pump would have under negative corona discharge has also been studied [138]. The apparatus had a diameter of 20 mm and reached a maximum air velocity of 1.7 m/s with an emitter voltage of -13 kV, while it displayed higher efficiency than that of a mechanical fan of equivalent diameter.

Other studies include a saw-tooth emitter to mesh design, which has been experimentally tested and optimized, finally reaching a maximum exit air velocity of 1.6 m/s with a 12-kV 1.2-kHz ac voltage applied to the emitter [139] and a wire-to-plate system displaying the velocity profile of EHD flow enhancers in absence of external bulk airflow [140]. A newer study took a more complex approach, examining the properties of an EHD pump Fig. 6 with a wire-to-cylinder-to-plate electrode configuration [141]. In this paper, the emitter wire electrode of the pump was connected to a 14-kV voltage source, the middle cylinder electrodes were grounded, and the collector electrodes were connected to an adjustable 0- to -8-kV adjustable voltage source. This design essentially

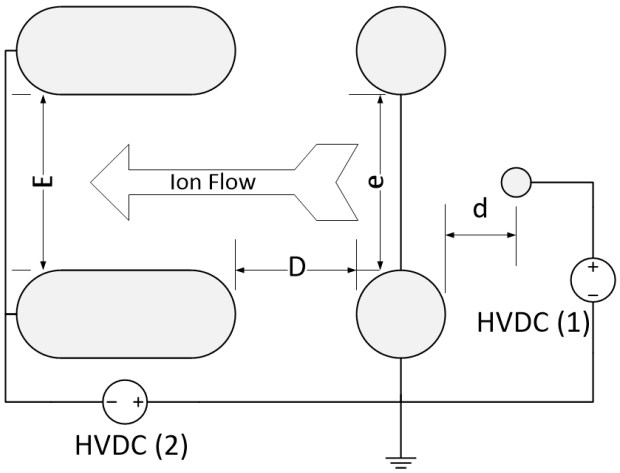

Fig. 6. Schematic view of the wire-to-cylinder-to-plate EHD pump presented in [141].

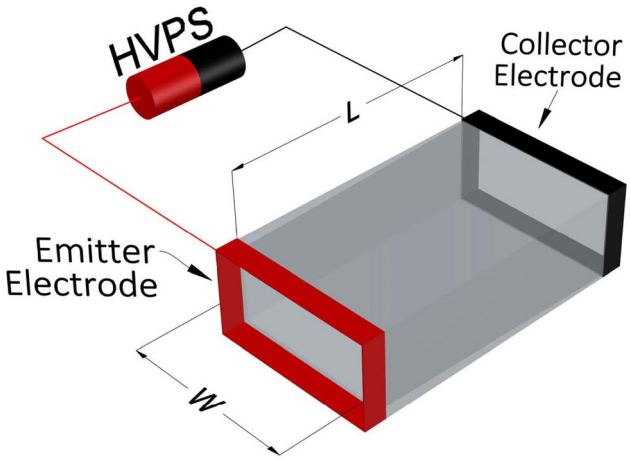

Fig. 7. EHD pump geometry that [149] used to determine the properties of different working fluids.

decoupled ionization and particle acceleration, using the wire emitter for ionization and the field developed between the cylinders and the plate for acceleration. The results were positive, displaying a mechanical power increase of up to 78% and an overall efficiency increase of 0.4% (from 0.9% to 1.3%) over wire-to-plate configurations.

Owsenek *et al*. [142] were one of the first to experiment with the direct applicability of a standalone EHD air pump, exploring the cooling performance of a simple needle-to-plane EHD pump, which increased heat transfer over free (passive) convection by 25 times. Similar studies have also been performed in [143], which reported an increased heat transfer rate of up to 250% using a wire-to-plane EHD pump, and [144], which reported an increased heat transfer rate of up to 200% using a wire-to-plane EHD pump inside a confined area. A more recent application study has also been performed, for the design of an EHD pump driving a sampling system to be installed on a vehicle to be sent to Mars, experimenting with the prototype in earth conditions and discussing the changes that will apply on the much different environment of another planet [145]. Researchers also explored a distinct advantage offered by EHD pumps that of scaling. EHD pumps have no moving parts, therefore fabrication to a scale of μm or even lower is possible. The first to explore such a possibility were Bart *et al*. [146] and other researchers soon followed [147]. The authors used opposed electrode grids and were able to pump most organic solvents. Richter and Sandmaier [147] also described that there is a correlation between the electrode distance and the driving voltage, as well as mentioned that the stacking of several EHD micropumps is a possibility for increased pressure. A wire-to-plate EHD micropump was also presented a few years later, with the prototype reaching an air flow of up to 4 mm/s [148].

Aside from EHD air pumps, [149] was the first to publish an experimental study on the behavior of multiple working fluids using a simple rectangular duct EHD pump with a parallel strip-to-strip electrode geometry (Fig. 7). This paper listed the maximum velocity and efficiency of no less than 20 working fluids, concluding that there are vast differences on the maximum velocity that different fluids may achieve, ranging from 0.38 to 6.62 m/s in this particular study, as well as that the maximum efficiency is not dependent on the maximum velocity of a given fluid. Among the first studies regarding the use of a medium other than air has been performed in [150], which explored the direct application of EHD pumps inside a transformer. Their results were promising but not practical, as the generated liquid flow of about 9.5 cm/s was satisfactory but the collector electrode, which also acted as a filter, was soiled by residue after a few hundred hours of operation. Many years later, a multistage EHD pump design was presented with transformer oil being the working fluid, suggesting that EHD pumps could become a practical solution for the cooling of electrical machinery [151], [152]. An experimental research using a wire-to-wire EHD pump has also been presented, using dielectric fluid (Dibutyl Sebacate, an organic plasticizer) as the medium, both as a single stage [153] and as a multiple stage configuration of the same geometry [154]. Fuhr *et al.* [155] also explored the viability of pumping high-conductivity fluids, as well as water solutions [156] and, by performing experiments with an EHD micropump using a multiple plane to plane electrode geometry, proved that the practicality of EHD pumping is not limited to low-conductivity fluids, concluding that it could have significant applications in bioscience and on chemical engineering. For application to cryogenics, an EHD micropump design using liquid nitrogen as the cooling medium has also been presented [157]. The saw-tooth emitter to plane collector EHD micropump achieved a flow rate of 2.3 gr/min and a pressure head of 5 Pa with 1 kV applied to the emitter. A few years later, it received a design upgrade and the pressure head reached 13 Pa with a 50-μm electrode spacing and 1 kV applied to the emitter, while a pumping head of up to 26 Pa with 650 V applied to the emitter proved to be possible but at a reduced 20-μm electrode spacing and over twice the number of pumping stages [158]. Table III summarizes the research results on EHD air pumps to this date.

B. EHD Pumps Designed for Semiconductor Cooling

Even though the first fabricated and experimentally tested EHD micropump design is considered to be that of [147], development of EHD pumps specifically for cooling purposes

TABLE III
REPORTED PERFORMANCE OF EHD AIR PUMP DESIGNS

Author	Electrode Geometry	Velocity measurement method	Fluid velocity	Efficiency
Moreau and Touchard [119]	Needle-to-grid	Pitot tube 2 mm after collector electrode	8 m/s max (d=15 mm, Id=12 μA, positive corona)	1.72% max (d=1.7 mm, Id=12μA)
Moon et al. [121]	Needle/ring-to-grid	Anemometer 10 mm after collector electrode	4.54 m/s max (d=15 mm, V=+15 kV)	7.25% (d=15 mm, V=+15 kV)
Moon et al. [127]	Needle-to-grid	Anemometer 35 mm after collector electrode	2.75 m/s max (d=15 mm, V=-19 kV)	≈0.934% max (d=15 mm, V=+18 kV)
Kim et al. [122]	Needles-to-ring, 1 to 6 stages	Hot-wire anemometer 34 mm after collector electrode	1 Stage: 2.5 m/s max (V=29.8 kV) 6 Stages: 6 m/s max (V=29.8 kV)	1 Stage: 0.38% max (V=29.8 kV) 6 Stages: 0.92% max (V=29.8 kV)
Rickard et al. [125]	Needle-to-ring	Particle image velocimetry 3 mm after the collector electrode	1.2 m/s mean, 2.1 m/s max (d=9.5 mm, V=10.3 kV)	≈0.0245% (d=9.5 mm, V=10.3 kV, Id=71.6μA)
Nakamura and Ohyama [128]	Needle-to-ring	Particle image velocimetry	1.6 m/s mean (d=10 mm, V=10 kV)	≈0.0167% (d=10 mm, V=10 kV, Id=5μA)
Qiu et al. [129]	Needles-to-mesh, 1 to 5 stages	Anemometer 2 mm after the collector electrode	1 stage: 4.9 m/s mean (d=13 mm, V=17 kV) 4 stages: 7.39 m/s mean (d=8.5 mm, V=33 kV)	1 stage: ≈0.65% 4 stages: ≈0.8%
Wei et al. [130]	Needles-to-mesh, 1 to 33 stages	Anemometer 2 mm after the collector electrode	1 stage: 4.4 m/s mean (d=11 mm, V=-13 kV) 25 stages: 16.1 m/s mean (d=11 mm, V=33 kV)	1 stage: ≈0.55% (d=11 mm, V=-9 kV) 25 stages: ≈2.2% (d=11 mm, V=-9 kV)
Zhao and Adamiak [131]	Needle-to-mesh	Hot wire anemometer 1.6 mm after the collector electrode	4.1 m/s max (d=20 mm, V=13 kV)	No current or power information disclosed
Karakas et al. [133]	Needles-to-mesh	Anemometer 50 mm after the collector electrode	1.75 m/s mean (d=30 mm, V=30 kV)	No current or power information disclosed
Zhang and Lai [135]	Wire/Needles-to-ring	Hot-wire anemometer 25.4 mm after the collector electrode	0.8 m/s mean (d=3.8 mm, V=30 kV)	36 L/sW (V=20 kV) 4 L/sW (V=28 kV)
Komeili et al. [137]	Wire-to-cylinder	Hot-wire anemometer 8 mm after the collector electrode	1.9 m/s mean (V=-16 kV, d=12.6 mm)	≈0.3644% (V=-16 kV, d=12.6 mm)
Takeuchi and Yasuoka [138]	Wire-to-Cylinder	Hot-wire anemometer 145 mm after the collector electrode	1.7 m/s mean (V=-13 kV, d=13 mm)	≈1% max (V=-13 kV, d=13 mm)
Moon et al. [139]	Needles-to-grid	Anemometer 10 mm after collector electrode	1.65 m/s mean (V=12.4 kV A/C, f=1.2 kHz, d=12.6 mm)	<0.001%
Colas et al. [141]	Wire-to-cylinder-to-plate	Pitot tube 2mm after collector electrode	7m/s to 9m/s max (V=14 kV, d=3 mm)	0.9% (no secondary acceleration) to 1.3% (with secondary acceleration)

*Where d is the distance between the collector and emitter electrodes, Id is the corona discharge current and V is the voltage applied to the emitter.

began with the presentation of a micropump designed for integration in microelectromechanical systems [159]. The EHD micropump was developed using laser micromachining technology and was capable of inducing a pressure head of 287 Pa with the application of 120 V over a 50-μm spacing with propanol being the working fluid. During the same period, a similar, relatively simple EHD micropump using parallel planar electrodes, was tested by another research team, using ethyl alcohol as the heat transfer working medium [160]. Another similar micropump was developed and fabricated a few years later in [161] for the exact same purpose, using R-134a as the working fluid and capable of supplying a pressure head of 250 Pa with the application of 150 V over a 50-μm spacing. Soon afterward, a research team led by the same author investigated the performance of different electrode geometries, comparing the performance of an EHD micropump, based on the simple parallel planar electrode design, against designs, which introduced saw-tooth emitter electrodes [162]. The team derived that the saw-tooth emitter electrode design could yield a significantly higher pressure

head and with a notably lower voltage applied to the emitter, reaching a pressure head of about 750 Pa with a power consumption of 4 mW and a distance of 50 μm between the electrodes, while the parallel planar electrode design required over 80 mW to reach a pressure head of 580 Pa over the same distance. During the same year, a similar pump with HFE-7100 as the working fluid but with significantly better performance at lower voltages was presented [163].

A further improvement of the design has been presented a few years later, with a chip-integrated cooling device capable of reaching a cooling rate up to 35 $W \cdot cm^2$ and which could yield a static pressure of 320 Pa, but which also required a voltage of 400 V over a distance of 20 μm to reach those figures [164]. Another similar design for chip-integrated cooling demonstrated that a pressure head of 700 Pa with the application of 450 V over a 20-μm spacing is also possible, again with HFE-7100 as the working fluid [165]. Aside from EHD micropumps using parallel planar and saw tooth-to-planar electrode designs, an EHD micropump with a parallel micropillar electrode design has also been presented, which displayed significantly increased performance, reaching a static pressure of 620 Pa with an applied voltage of 300 V and a 40-μm distance between the electrodes [166]. A more recent study of an EHD micropump, again with parallel planar electrodes and using HFE-7100 as the working fluid, displayed that a pressure head of 268 Pa is possible with only 90 V if the emitter electrode is made of gold instead of copper [167]. The same design with a copper electrode required over twice the voltage to produce the same performance.

Darabi and Rhodes [168] have also published a paper specifically focused on the CFD modeling of EHD micropumps. This paper presented a 2-D numerical model of a cross section of the device, which was based on the assumptions that:

1) the flow is laminar, linear, and incompressible;
2) the electrodes are planar strips on the bottom substrate;
3) there is no end effect on either side of the channel;
4) there is only one type of ion present in the liquid.

The model displayed very good fit against experimental data derived from a micropump, which had been previously fabricated and tested by the same author [162]; however, 2-D modeling is ineffective for the numerical analysis of more complex EHD micropump geometries. Table IV summarizes the research results on experimentally tested EHD micropumps to this date.

The first experimental approach on the cooling of high power density electronic chips implementing ionic wind took place in Israel a decade ago [169], examining a wire-to-plate (wings) electrode configuration (Fig. 8).

The particular configuration had the advantage of being isolated from the cooled components; therefore, the components would not have to be constructed from metallic materials and would not be subjected to a strong electric field. The author determined the optimal angles and dimensions ($a = b = 90°$, $\theta = 34.5°$, and $H = 50$ mm) for this particular configuration. It was determined that the heat transfer rate has been augmented three times over the free convection heat transfer coefficient. The author also suggested that ionic wind blowers can be used for cooling electronic components and acclaimed their noiseless operation and high reliability. Unfortunately, although the author clearly mentioned that the ionic wind generator requires high power, no results regarding the electrical to mechanical energy conversion efficiency and/or power consumption of the system were presented.

Soon afterward, a needle-to-vertical plate electrode design EHD air pump, designed for cooling of high power density electronic chips, was presented [170]. The authors used an experimental setup and determined several aerodynamic and key performance characteristics. Under 11-kV electrode voltage, the experimental setup managed to reach an average air velocity of about 3.0 m/s over a diameter of 60 mm and a maximum velocity of 4.1 m/s, performance figures greater than several of the mechanical blowers available at the time; however, the energy conversion efficiency was lower than 0.35 CFM/W. According to the same study, a rotary mechanical fan of similar (3.4 m/s) output velocity had an efficiency of 7.78 CFM/W, more than 22 times higher. However, the authors also determined that increasing the corona electrode voltage further had minimal impacts on efficiency, while the air velocity remained linearly dependent on the corona electrode voltage, implying that higher voltage would increase air velocity without a significant reduction of energy efficiency. In this paper, it was also determined that as the emitter electrode voltage increases beyond the corona onset voltage, the collector electrode current grows exponentially, which is known to reduce the efficiency of the system. The outcome of this research, in conjunction with the discovery that conversion efficiency also improves as the velocity of the air increases [123], indicates that there might be good development potential for multiple stage EHD pumps. Three years later, a part of the same team published a detailed paper on how their initial model has been designed and optimized, as well as simulations and optimization techniques for EHD pumps in general [171]. Schlitz and Singhal [172] also experimentally tested several prototypes of different electrode configurations and suggested specific designs for integration into mobile devices and general use on electronic chips. The best design presented, using multiple wires as emitter electrodes and multiple wavy fins as collector electrodes, reached an average air velocity of 1.6 m/s with a configuration allegedly compact enough to fit inside a laptop; however, the exact measurements of the device were not made known.

The first practical application of utilizing an EHD pump to cool high power density electronic components was introduced in early 2009, with an EHD pump retrofitted inside a laptop [173]. The experimental pump utilized a wire-to-dual plate design, with the grounded collector electrodes acting as the electronic chip heat sinks; therefore, the heat is drawn from the electronic chip on the collector electrode, which in turn is removed by the ionic wind generated by the configuration (Fig. 9). Unfortunately, this paper did not disclose thorough experimental data, most likely because the company intended the commercialization of the design, as it can be derived from the multitude of patents which soon followed (see [174]–[176]). This paper stated that the electronic high-voltage power supply had been installed into the mechanical fan cavity

TABLE IV
SUMMARIZED PERFORMANCE OF EXPERIMENTALLY TESTED EHD MICROPUMPS

Author	Working medium	Electrode Spacing	Pressure head
Richter and Sandmaier [147]	Ethanol	140 μm	600 Pa at 280 V
			1250 Pa at 480 V
			2480 Pa at 700 V
Wong et al. [159]	Propanol	50 μm	45 Pa at 60 V
			150 Pa at 90 V
			287 Pa at 120 V
Si-Hong and Yong-Kweon [160]	Ethyl alcohol	100 μm	45 Pa at 40 V
			120 Pa at 70 V
			245 Pa at 110 V
Darabi et al. [161]	R-134a	50 μm	40 Pa at 50 V
			120 Pa at 100 V
			250 Pa at 150 V
Chowdhury et al. [163]	HFE-7100	20 μm	50 Pa at 40 V
			145 Pa at 80 V
			190 Pa at 120 V
Chowdhury et al. [163]	HFE-7100	100 μm	45 Pa at 200 V
			125 Pa at 300 V
			175 Pa at 350 V
Darabi et al. [162]	HFE-7100	50 μm	Planar emitter:
			100 Pa at 600 V
			175 Pa at 750 V
			580 Pa at 1000 V
			Sawtooth emitter:
			50 Pa at 130 V
			200 Pa at 200 V
			700 Pa at 250 V
Darabi and Ekula [164]	HFE-7100	20 μm	60 Pa at 100 V
			180 Pa at 250 V
			320 Pa at 400 V
Benetis et al. [165]	HFE-7100	20 μm	220 Pa at 200 V
			300 Pa at 300 V
			660 Pa at 450 V
Benetis et al. [165]	HFE-7100	50 μm	250 Pa at 200 V
			380 Pa at 300 V
			600 Pa at 500 V
Lee et al. [166]	HFE-7100	40 μm	160 Pa at 150 V
			250 Pa at 200 V
			640 Pa at 300 V
Yu et al. [167]	HFE-7100	20 μm	120 Pa at 50 V (Au electrode)
			268 Pa at 90 V (Au electrode)
			230 Pa at 200 V (Cu electrode)
Zhao and Lawler [157]	LN2	50 μm	≈5 Pa at 1000 V
Foroughi et al. [158]	LN2	20 μm	22 Pa at 500 V
			26 Pa at 650 V

alongside the EHD air pump, yet no data on the power supply specifications, voltage and/or current output, and/or the electrical to mechanical energy conversion efficiency of the system were given. Only temperature comparison data between the stock mechanical fan and the EHD air pump has been shared, with the EHD air pump appearing able to deliver similar performance to that of the stock cooling fan. Since the laptop was a commercial product, which had been retrofitted, the cooling system understandably was designed to optimize the performance of the stock mechanical fan. After receiving such results, the authors decided to further improve the EHD air pump by removing the constraints of fitting the EHD system inside the mechanical fan's cavity. No more information than that was given on this new design.

A similar study has been performed at the University of Purdue, assessing the possibility of exploiting the ionic wind phenomenon to help in improving the cooling of smaller electronic chips, mainly used in portable platforms [68]. Although the research team emphasized their research on enhancing fluid flows generated by mechanical fans, this particular study also included the performance results without an existing air stream over a wire-to-ribbon electrode configuration

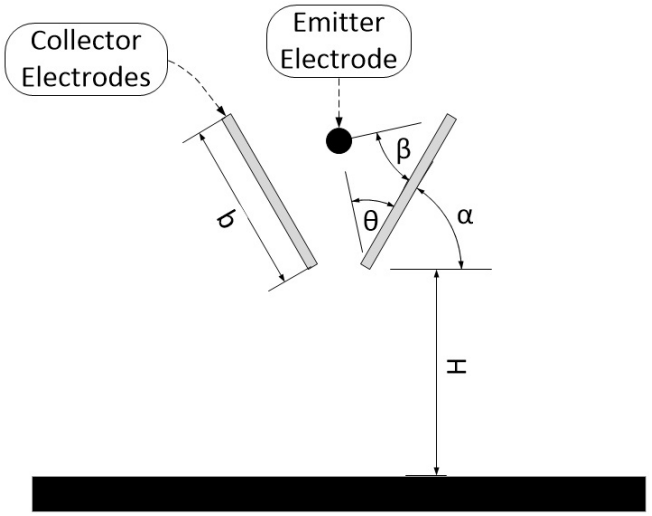

Fig. 8. Geometry of the wire-to-wing electric blower (indicative of the geometry under study in [169], not in proportion with the optimal configuration).

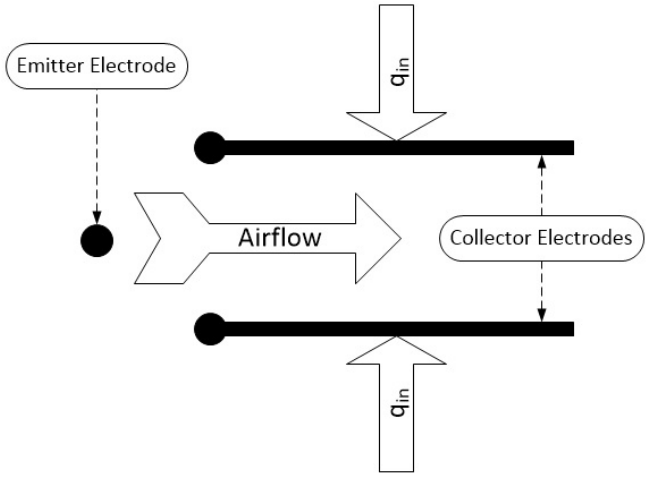

Fig. 9. Geometry of the laptop EHD pump developed in [173].

EHD pump. The experiments were conducted by heating the 14.5-cm^2 substrate with the use of a thin-film heater producing 1375 W/(K $\cdot$ m^2) and the study derived that the ionic wind was capable of enhancing the flow generated by a mechanical fan and decrease the temperature rise over the ambient by 2 °C–3 °C, limiting it to 28 °C above ambient; however, the EHD pump alone could cool the quartz substrate and limit the temperature rise over the ambient to 40 °C without the presence of a mechanical fan, reaching a performance comparable with that of the standard fan-based cooling system. According to the research results, this experimental EHD pump was capable of cooling a chip with a thermal design power value of 2 W while draining a mere 16.4 mW.

A wire-to-plate EHD pump of capillary design has also been proposed for the cooling of microelectronics, with the experimental prototype, which was 35-mm tall and 17.6-mm wide, reaching a maximum exit wind speed of 1.7 m/s at 8.4 kV [177], [178]. The diameter of the pump outlet, however, was only 5 mm, thus the average exit wind speed of the device may considerably degrade over larger diameters.

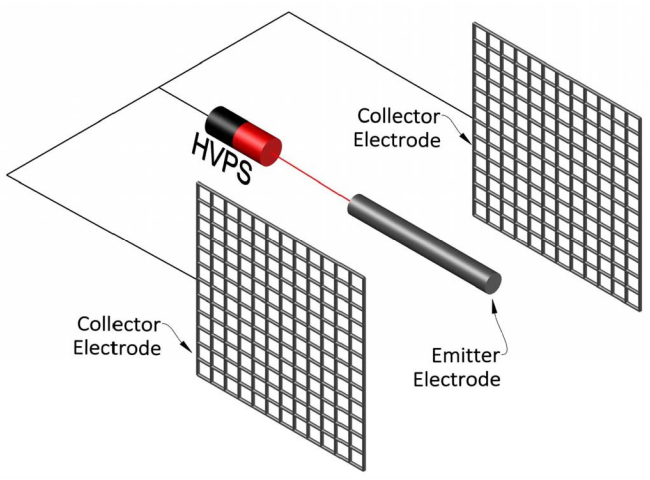

Fig. 10. Rod-to-mesh electrode design presented in [179].

An EHD pump based on a rod-to-mesh electrode design (Fig. 10) and making use of a negative corona discharge has also been presented [179]. It was noted that positive corona gave inferior performance results with that particular configuration. After the optimization of their design, the authors noted that the experimental EHD pump reached a coefficient of performance of 26.5 with just −760 V but no results regarding the wind velocity have been presented.

Recently, another study examined the exploitation of multiple electrode configurations for the cooling of light-emitting diodes [180]. All of the configurations utilized a needle emitter electrode but the collector electrode was either a needle, a line (wire), or a mesh. Positive and negative coronas were also tested, with the authors indicating that a positive corona discharge is more efficient and offers better performance, even though the operational range is slightly narrower. With thermal resistance being the sole benchmarking factor, the experimental setup using a mesh collector electrode displayed the best performance, which slightly increased for smaller mesh apertures.

Only one study has been presented on reliability concerns with EHD cooling systems. A primary concern regarding EHD-based cooling systems is dust, since the collector electrode displays behavior similar to that of a high-voltage ESP. Jewell–Larsen *et al*. [181] investigated the amount and characteristics of dust collected by a novel EHD system, similar to the one the team had proposed a few years earlier for cooling laptop computers. The study concluded that the majority of the dust was collected in two locations on the collector plate, with the high percentage of large dust particles (above 10 μm) collected on the first half of the collector. Although the accumulation of particles is desired in EHD devices designed for other purposes, such as precipitators and air cleaners [182], the accumulation of dust on the collector of a cooling device, and or the body that requires cooling itself, has a degrading effect on the longevity and performance of the EHD device. Regrettably, the study itself offers no advice on how to reduce the accumulation of dust. Nevertheless, the simulations developed are valuable for investigating and optimizing the longevity of EHD pumps.

VII. Conclusion

Today, EHD is rapidly evolving as a scientific discipline with immense research potential in multiple disciplinary fields. Industrially, EHD has practical applications in several businesses, such as in food, pharmaceutical, mechanical, space, and electronic industries.

The development of EHD thrusters is still at an early stage. As they are considered to be the only currently viable solution for long-term space travel, research on EHD thrusters is mostly being performed for use in space, generally by organizations related to the exploration of space and the control of satellites. Research on atmospheric thrusters has been very slow and mostly around the Ionocrafts presented nearly a century ago. Advancing and improving the performance of EHD thrusters has great research headroom, especially on the control of the field geometry order to reduce cosine losses from particle collision momentum transfers.

Significant research has been performed to explore the effect that EHD flows would have on the boundary layer, for both the reduction of drag and for the enhancement of heat transfer via convection. The heat transfer enhancement ratio for several working mediums has been explored; however, the number of configurations which remains unexplored is immense, as is the possibility of further augmentation via the application of ac or pulsed dc instead of simple dc voltage. Research on the possible performance enhancement that the reduction of drag could offer to specific widely used engineering applications, such as airplanes and wind turbines, could also lead to the augmented performance and or reduced fuel consumption.

Research on EHD drying has been significant and it was proven that EHD drying can be a highly viable alternative to oven drying, especially for drying materials and food products sensitive to heat, reducing energy requirements, and dramatically enhancing the end quality of the products. However, research has almost been exclusively focused on the removal of water from the medium. There has been a little to no research on the interaction of the charged particles with the biochemical substances of nutrients. Furthermore, the vast majority of the experimental studies has been performed using simple needle-to-plane configurations; as such, there is a large research headroom on the development of more advanced electrode configurations and or experimentally exploring the performance of electrode configurations presented in the past years. Finally, there have been virtually no studies comparing the performance of EHD dryers to RF dryers, which should also be explored.

Most of the recent research on practical devices based on the EHD effect has been focused on designing fluid accelerators (pumps), which may then be used on a wide variety of applications, the most notable of which being drying and cooling. There have been numerous experimental studies on various electrode configurations, yet there are several configurations, which ought to be explored, such as the use of ac or pulsed dc voltage and the performance of cascading electrode configurations. Due to their scaling ability, EHD pump configurations appear ideal for use in confined spaces, very small electronic devices and even as standalone on-chip cooling solutions; therefore, there also is a great research opportunity on how the performance characteristics of known and or new electrode geometries scale in relation to their physical size.

References

[1] N. Cabeo, *Philosophia Magnetica*. Cologne, Germany: Francesco Suzzi, Ferrara, 1629.

[2] I. Newton, *Optics*. London, U.K.: Printed for Sam. Smith, and Benj. Walford, Printers to the Royal Society, 1718.

[3] B. Wilson, *Treatise on Electricity*. Washington, DC, USA: C. Corbet, 1750.

[4] T. Cavallo, *A Complete Treatise of Electricity*. London, U.K.: Edward, 1777.

[5] M. Faraday, *Experimental Researches in Electricity*. Carlsbad, CA, USA: Faraday, 1834.

[6] J. C. Maxwell, *Treatise in Electricity and Magnetism*. Oxford, U.K.: Oxford Univ. Press, 1873.

[7] A. P. Chattock, "On the velocity and mass of the ions in the electric wind in air," *Phil. Mag.*, vol. 48, no. 294, pp. 401–420, 1899.

[8] F. W. Peek, *Dielectric Phenomena in High Voltage Engineering*. New York, NY, USA: McGraw-Hill, 1915.

[9] T. Musha, "Theoretical explanation of the biefeld-brown effect," *Electr. Spacecraft J.*, vol. 31, no. 1, pp. 21–29, 2000.

[10] M. Tajmar, "Biefeld-brown effect: Misinterpretation of corona wind phenomena," *AIAA J.*, vol. 42, no. 2, pp. 315–318, Feb. 2004.

[11] E. Lob, *Archiv Der Elektrischen Uebertragung*, Baden-Württemberg, Germany: Stuttgart, 1954.

[12] D. J. Harney, *An Aerodynamic Study of the Electric Wind*. Pasadena, CA, USA: California Inst. Technol., 1957.

[13] O. M. Stuetzer, "Magnetohydrodynamics and electrohydrodynamics," *Phys. Fluids*, vol. 5, no. 5, p. 534, 1962.

[14] R. D. Morrison and D. M. Hopstock, "The distribution of current in wire-to-cylinder corona," *J. Electrostat.*, vol. 6, no. 4, pp. 349–360, Sep. 1979.

[15] J. Argyris and D. Scharpf, "Finite elements in time and space," *Nuclear Eng. Des.*, vol. 10, no. 4, pp. 456–464, Dec. 1969.

[16] K. H. Huebner, *The Finite Element Method for Engineers*. New York, NY, USA: Wiley, 1975.

[17] J. L. Davis and J. F. Hoburg, "Wire-duct precipitator field and charge computation using finite element and characteristics methods," *J. Electrostatics*, vol. 14, no. 2, pp. 187–199, Aug. 1983.

[18] S. Cristina, G. Dinelli, and M. Feliziani, "Numerical computation of corona space charge and VI characteristic in DC electrostatic precipitators," *IEEE Trans. Ind. Appl.*, vol. 27, no. 1, pp. 147–153, Jan./Feb. 1991.

[19] D. Meeker. (2006). *Finite Element Method Magnetics (FEMM), Version 4.2* [Online]. Available: http://femm.berlios.de

[20] R. Morrow, "The theory of positive glow corona," *J. Phys. D, Appl. Phys.*, vol. 30, no. 22, p. 3099, Nov. 1997.

[21] G. Georghiou, R. Morrow, and A. Metaxas, "A two-dimensional, finite-element, flux-corrected transport algorithm for the solution of gas discharge problems," *J. Phys. D, Appl. Phys.*, vol. 33, no. 19, p. 2453, Oct. 2000.

[22] P. Atten, K. Adamiak, and V. Atrazhev, "Electric corona discharge simulation in the hyperbolic point—Ground plane configuration," in *Proc. Annu. Rep. Conf. Electr. Insul. Dielectr. Phenomena*, 2002, pp. 109–112.

[23] K. Adamiak and P. Atten, "Simulation of corona discharge in point-plane configuration," *J. Electrostatics*, vol. 61, no. 2, pp. 85–98, Jun. 2004.

[24] L. Zhao, E. D. Cruz, K. Adamiak, A. Berezin, and J. Chang, "A numerical model of a wire-plate electrostatic precipitator under electrohydrodynamic flow conditions," in *Proc. Int. Conf. Air Pollution Abatement Technol. Future Challenges*, 2006, pp. 1–9.

[25] J. Suda, T. Ivancsy, I. Kiss, and I. Berta, "Complex analysis of ionic wind in ESP modeling," in *Proc. 10th Int. Conf. Electrostatic Precipitator*, 2006, pp. 1–13.

[26] J. Balaji, S. Wei, and T. Siddharth, "Modeling of dielectric barrier discharge and resulting fluid dynamics," in *Proc. 44th AIAA Aerosp. Sci. Meeting Exhibit., Amer. Inst. Aeronautics Astron.*, 2006, pp. 1–20.

[27] D. B. Go, S. V. Garimella, and T. S. Fisher, "Numerical simulation of microscale ionic wind for local cooling enhancement," in *Proc. IEEE 10th Intersoc. Conf. Thermal Thermomech. Phenomena Electron. Syst.*, Jun. 2006, pp. 45–53.

[28] J. P. A. Bastos and N. Sadowski, *Electromagnetic Modeling by Finite Element Methods*. New York, NY, USA: Marcel Dekker, 2003.

[29] S. S. Rao, *The Finite Element Method in Engineering*. New York, NY, USA: Elsevier Sci., 2011.

[30] S. Moaveni, *Finite Element Analysis: Theory and Application with Ansys*. Englewood Cliffs, NJ, USA: Prentice-Hall, 1999.

[31] D. Meeker, *FEMM-Finite Element Method Magnetics*. Alpharetta, GA, USA: Aladdin Enterprise, Nov. 1999.

[32] P. Glushchenko and Y. K. Stishkov, "Modeling of the through EHD-flow structure in a wire-wire system," *Surf. Eng. Appl. Electrochem.*, vol. 43, no. 4, pp. 257–264, Aug. 2007.

[33] L. M. Dumitran, L. Dascalescu, P. V. Notingher, and P. Atten, "Modelling of corona discharge in cylinder-wire-plate electrode configuration," *J. Electrostatics*, vol. 65, no. 12, pp. 758–763, Nov. 2007.

[34] K. N. Kiousis and A. X. Moronis, "Experimental investigation of EHD flow in wire to cylinder electrode configuration," in *Proc. 10th IASTED Eur. Conf. Power Energy Syst.*, 2011, pp. 21–26.

[35] Y. K. Stishkov and V. Chirkov, "Computer simulation of EHD flows in a needle-plane electrode system," *Tech. Phys.*, vol. 53, no. 11, pp. 1407–1413, Nov. 2008.

[36] T. T. Brown, "Electrokinetic apparatus," U.S. Patent 2 949 550, Aug. 16, 1960.

[37] T. T. Brown, "Electrokinetic transducer," U.S. Patent 3 018 394, Jan. 23, 1962.

[38] T. T. Brown, "Electrokinetic apparatus," U.S. Patent 3 187 206, Jun. 1, 1965.

[39] A. P. D. Seversky, "Ionocraft," U.S. Patent 3 130 945, Apr. 31, 1964.

[40] E. A. Christenson and P. S. Moller, "Ion-neutral propulsion in atmospheric media," *AIAA J.*, vol. 5, no. 10, pp. 1768–1773, Oct. 1967.

[41] Scythe INC. Toronto, ON, Canada. (2013, Jul. 13). *Scythe Mini Kaze Ultra 40 x 20 mm Fan Specifications* [Online]. Available: http://www.scythe-usa.com/product/acc/023/sy124020l_detail.html

[42] Yate Loon Electronics Co. Ltd. Taipei, Taiwan. (2013, Jul. 13). *Yate Loon D60SM-12C 60 × 20 mm Fan Specifications* [Online]. Available: http://www.yateloon.com/style/content/CN-02c/product_detail.asp?lang=2&customer_id=1356&name_id=31277&rid=58936&id=38826

[43] A. Morozov and L. Solov'ev, "Motion of charged particles in electromagnetic fields," *Rev. Plasma Phys.*, vol. 2, no. 1, p. 201, 1966.

[44] J. S. Sovey and M. A. Mantenieks, "Performance and lifetime assessment of magnetoplasmadynamic arc thruster technology," *J. Propuls. Power*, vol. 7, no. 1, pp. 71–83, Jan. 1991.

[45] F. S. Gulczinski and R. A. Spores, "Analysis of Hall-effect thrusters and ion engines for orbit transfer missions," in *Proc. 32nd Joint Propuls. Conf. Exhibit.*, 1996, pp. 1–18.

[46] S. Marcuccio, A. Genovese, and M. Andrenucci, "Experimental performance of field emission microthrusters," *J. Propuls. Power*, vol. 14, no. 5, pp. 774–781, Sep. 1998.

[47] L. F. Velasquez-Garcia, A. I. Akinwande, and M. Martinez-Sanchez, "A planar array of micro-fabricated electrospray emitters for thruster applications," *J. Microelectromech. Syst.*, vol. 15, no. 5, pp. 1272–1280, Oct. 2006.

[48] F. X. Canning, C. Melcher, and E. Winet, "Asymmetrical capacitors for propulsion," Inst. Sci. Res., NASA, Washington, DC, USA, Tech. Rep. CR-2004-213312, Oct. 2004.

[49] L. Zhao and K. Adamiak, "EHD gas flow in electrostatic levitation unit," *J. Electrostatics*, vol. 64, no. 7, pp. 639–645, Jul. 2006.

[50] C. F. Chung and W. J. Li, "Experimental studies and parametric modeling of ionic flyers," in *Proc. IEEE/ASME Int. Conf. Adv. Intell. Mechatron.*, Sep. 2007, pp. 1–6.

[51] L. Koziell, L. Zhao, J. Liaw, and K. Adamiak, "Experimental studies of EHD lifters," in *Proc. ESA Annu. Meeting Electrostatics*, Jun. 2011, pp. 1–6.

[52] C. Wan, "Electro-hydrodynamic (EHD) thruster analysis and optimization," M.S. thesis, Albert Nerken School Eng., Cooper Union, New York, NY, USA, 2009.

[53] J.-M. Wang, T.-Y. Lin, and L.-J. Yang, "Electrohydrodynamic (EHD) micro-boat," in *Proc. IEEE 2nd IEEE Int. Conf. Nano/Micro Eng. Molecular Syst.*, Jan. 2007, pp. 584–587.

[54] H. S. Poon, M. K. Lam, M. Chow, and W. J. Li, "Noiseless and vibration-free ionic propulsion technology for indoor surveillance blimps," in *Proc. IEEE Int. Conf. Robot. Autom.*, May 2009, pp. 2891–2896.

[55] L. Pekker and M. Young, "Model of ideal electrohydrodynamic thruster," *J. Propuls. Power*, vol. 27, no. 4, pp. 786–792, 2011.

[56] J. Wilson, H. D. Perkins, and W. K. Thompson, *An Investigation of Ionic Wind Propulsion*. Washington, DC, USA: Nat. Aeronautics Space Admin., 2009.

[57] K. Masuyama, "Performance characterization of electrohydrodynamic propulsion devices," M.S. thesis, Dept. Aeronautics Astronautics, Massachusetts Inst. Technol., Boston, MA, USA, 2012.

[58] E. K. Levy, "The effects of electrostatic fields on forced convection heat transfer," Ph.D. dissertation, Dept. Mech. Eng., Massachusetts Inst. Technol., Minneapolis, MN, USA, 1964.

[59] J. L. Fernandez, "Electrohydrodynamic enhancement of forced convection heat transfer in tubes," Ph.D. dissertation, Dept. Mech. Eng., Univ. Bristol, Bristol, U.K., 1975.

[60] J. Fernández and R. Poulter, "Radial mass flow in electrohydrodynamically-enhanced forced heat transfer in tubes," *Int. J. Heat Mass Transf.*, vol. 30, no. 10, pp. 2125–2136, Oct. 1987.

[61] M. M. Ohadi, D. A. Nelson, and S. Zia, "Heat transfer enhancement of laminar and turbulent pipe flow via corona discharge," *Int. J. Heat Mass Transf.*, vol. 34, nos. 4–5, pp. 1175–1187, Apr. 1991.

[62] R. B. Lakeh and M. Molki, "Targeted heat transfer augmentation in circular tubes using a corona jet," *J. Electrostatics*, vol. 70, no. 1, pp. 31–42, Feb. 2012.

[63] J. Mathew and F. C. Lai, "Enhanced heat transfer in a horizontal channel with double electrodes," in *Proc. IEEE Conf. Rec. Ind. Appl. Conf., 13th IAS Annu. Meeting*, Oct. 1995, pp. 1472–1479.

[64] N. Kasayapanand and T. Kiatsiriroat, "EHD enhanced heat transfer in wavy channel," *Int. Commun. Heat Mass Transf.*, vol. 32, no. 6, pp. 809–821, May 2005.

[65] L. Léger, E. Moreau, G. Artana, and G. Touchard, "Influence of a DC corona discharge on the airflow along an inclined flat plate," *J. Electrostatics*, vol. 51, pp. 300–306, May 2001.

[66] L. Léger, E. Moreau, and G. G. Touchard, "Effect of a DC corona electrical discharge on the airflow along a flat plate," *IEEE Trans. Ind. Appl.*, vol. 38, no. 6, pp. 1478–1485, Nov. 2002.

[67] E. Moreau, L. Léger, and G. Touchard, "Effect of a DC surface-corona discharge on a flat plate boundary layer for air flow velocity up to 25 m/s," *J. Electrostat.*, vol. 64, no. 3, pp. 215–225, Mar. 2006.

[68] D. B. Go, R. A. Maturana, T. S. Fisher, and S. V. Garimella, "Enhancement of external forced convection by ionic wind," *Int. J. Heat Mass Transf.*, vol. 51, nos. 25–26, pp. 6047–6053, Dec. 2008.

[69] M. Robinson, "Convective heat transfer at the surface of a corona electrode," *Int. J. Heat Mass Transf.*, vol. 13, no. 2, pp. 263–274, Feb. 1970.

[70] T. Mizushina, H. Ueda, T. Matsumoto, and K. Waga, "Effect of electrically induced convection on heat transfer of air flow in an annulus," *J. Chem. Eng. Japan*, vol. 9, no. 2, pp. 97–102, 1976.

[71] H. Velkoff and R. Godfrey, "Low-velocity heat transfer to a flat plate in the presence of a corona discharge in air," *J. Heat Transf.*, vol. 101, no. 1, pp. 157–163, 1979.

[72] Y. Tada, A. Takimoto, and Y. Hayashi, "Heat transfer enhancement in a convective field by applying ionic wind," *J. Enhanced Heat Transf.*, vol. 4, no. 2, pp. 71–86, 1997.

[73] D. Nelson, M. Ohadi, S. Zia, and R. Whipple, "Electrostatic effects on heat transfer and pressure drop in cylindrical geometries," in *Proc. ASME/JSME Thermal Eng. Joint Conf.*, Reno, Nevada, Mar. 1991, pp. 33–39.

[74] M. M. Ohadi, "Heat transfer enhancement in heat exchangers," *ASHRAE J.*, vol. 33, no. 12, pp. 42–50, 1991.

[75] R. A. Moss and J. Grey, "Heat transfer augmentation by steady and alternating electric fields," in *Proc. Heat Transf. Fluid Mech. Inst.*, Santa Clara, CA, USA, Stanford University Press, Jun. 1966, pp. 210–235.

[76] R. H. Velkoff, "The effects of ionization on the flow and heat transfer of a dense gas in a transverse electrical field," in *Proc. Heat Transf. Fluid Mech. Inst.*, 1964, p. 260.

[77] F. Grosu and M. Bologa, "The influence of electric fields on heat-exchange processes in gases," *Appl. Electr. Phenom. USSR*, vol. 5, no. 23, pp. 350–356, 1968.

[78] H. Choi, "Electrohydrodynamic condensation heat transfer," *J. Heat Transf.*, vol. 90, pp. 98–102, Feb. 1968.

[79] A. Seth and L. Lee, "The effect of an electric field in the presence of noncondensable gas on film condensation heat transfer," *J. Heat Transf.*, vol. 96, no. 2, pp. 257–258, 1974.

[80] R. E. Holmes and A. Chapman, "Condensation of Freon-114 in the presence of a strong nonuniform, alternating electric field," *J. Heat Transf.*, vol. 92, no. 4, pp. 616–620, Nov. 1970.

[81] C. Damianidis, M. Collins, T. Karayiannis, and P. Allen, "EHD effect in condensation of dielectric fluids," in *Proc. 2nd Int. Symp. Condensers Condensat.*, Bath, U.K., 1990, pp. 505–518.

[82] T. Karayiannis, "EHD boiling heat transfer enhancement of R123 and R11 on a tube bundle," *Appl. Thermal Eng.*, vol. 18, nos. 9–10, pp. 809–817, Sep. 1998.

[83] J. Bryan and J. Seyed-Yagoobi, "Electrohydrodynamically enhanced convective boiling: Relationship between electrohydrodynamic pressure and momentum flux rate," *J. Heat Transf.*, vol. 122, no. 2, pp. 266–277, 2000.

[84] Y. Feng and J. Seyed-Yagoobi, "Mechanism of annular two-phase flow heat transfer enhancement and pressure drop penalty in the presence of a radial electric field-turbulence analysis," *J. Heat Transf.*, vol. 125, no. 3, pp. 478–486, 2003.

[85] H. Sadek, C. Y. Ching, and J. Cotton, "The effect of pulsed electric fields on horizontal tube side convective condensation," *Int. J. Heat Mass Transf.*, vol. 53, nos. 19–20, pp. 3721–3732, Sep. 2010.

[86] J. H. Davidson and P. J. McKinney, "EHD flow visualization in the wire-plate and barbed plate electrostatic precipitator," *IEEE Trans. Ind. Appl.*, vol. 27, no. 1, pp. 154–160, Jan./Feb. 1991.

[87] W.-J. Liang and T. H. Lin, "The characteristics of ionic wind and its effect on electrostatic precipitators," *Aerosol Sci. Technol.*, vol. 20, no. 4, pp. 330–344, 1994.

[88] A. Niewulis, J. Podlinski, V. Shapoval, and J. Mizeraczyk, "Collection efficiency in narrow electrostatic precipitators with a longitudinal or transverse wire electrode," *IEEE Trans. Dielectr. Electr. Insul*, vol. 18, no. 5, pp. 1423–1428, Oct. 2011.

[89] H. Fujishima, Y. Morita, M. Okubo, and T. Yamamoto, "Numerical simulation of three-dimensional electrohydrodynamics of spiked-electrode electrostatic precipitators," *IEEE Trans. Dielectr. Electr. Insul.*, vol. 13, no. 1, pp. 160–167, Feb. 2006.

[90] K. Adamiak and P. Atten, "Numerical simulation of the 2-D gas flow modified by the action of charged fine particles in a single-wire ESP," *IEEE Trans. Dielectr. Electr. Insul.*, vol. 16, no. 3, pp. 608–614, Jun. 2009.

[91] Z. Lin and K. Adamiak, "Numerical simulation of the electrohydrodynamic flow in a single wire-plate electrostatic precipitator," *IEEE Trans. Ind. Appl.*, vol. 44, no. 3, pp. 683–691, May/Jun. 2008.

[92] N. Farnoosh, G. S. P. Castle, and K. Adamiak, "A 3D simulation of a single section electrostatic precipitator for dust particles removal," in *Proc. 24th CCECE*, May 2011, pp. 000749–000752.

[93] T. Yamamoto, S. Maeda, Y. Ehara, and H. Kawakami, "Development of EHD-assisted plasma electrostatic precipitator," *IEEE Trans. Ind. Appl.*, vol. 49, no. 2, pp. 672–678, Mar./Apr. 2013.

[94] T. Yamamoto, S. Asada, and Y. Ehara, "Integrated diesel engine emission control using plasma combined hybrid system," in *Proc. IEEE IAS Annu. Meeting*, Oct. 2012, pp. 1–7.

[95] A. P. Krueger, W. W. Hicks, and J. C. Beckett, "Effects of unipolar air ions on microorganisms and on evaporation," *J. Franklin Inst.*, vol. 266, no. 1, pp. 9–19, Jul. 1958.

[96] N. N. Barthakur and S. Bhartendu, "Enhancement of evaporation rates from thin layers of liquids exposed to air ions," *Int. J. Biometeorol.*, vol. 32, no. 3, pp. 163–167, 1988.

[97] N. N. Barthakur, "An electrostatic method of drying saline water," *Dry. Technol.*, vol. 7, no. 3, pp. 503–521, Sep. 1989.

[98] N. N. Barthakur and T. Al-Kanani, "An electrohydrodynamic technique for removal of moisture from soil samples," *Commun. Soil Sci. Plant Anal.*, vol. 21, nos. 7–8, pp. 649–665, May 1990.

[99] Y. H. Chen and N. N. Barthakur, "Potato slab dehydration by air ions from corona discharge," *Int. J. Biometeorol.*, vol. 35, no. 2, pp. 67–70, Jun. 1991.

[100] N. N. Barthakur and N. P. Arnold, "Evaporation rate enhancement of water with air ions from a corona discharge," *Int. J. Biometeorol.*, vol. 39, no. 1, pp. 29–33, Mar. 1995.

[101] F. Lai, M. Huang, and D. Wong, "EHD-enhanced water evaporation," *Dry. Technol.*, vol. 22, no. 3, pp. 597–608, Jan. 2004.

[102] A. Alem-Rajabif and F. Lai, "EHD-enhanced drying of partially wetted glass beads," *Dry. Technol.*, vol. 23, no. 3, pp. 597–609, Mar. 2005.

[103] F. Hashinaga, T. R. Bajgai, S. Isobe, and N. N. Barthakur, "Electrohydrodynamic (EHD) drying of apple slices," *Dry. Technol.*, vol. 17, no. 3, pp. 479–495, Mar. 1999.

[104] T. R. Bajgai and F. Hashinaga, "Drying of spinach with a high electric field," *Dry. Technol.*, vol. 19, no. 9, pp. 2331–2341, Sep. 2001.

[105] W. Cao, Y. Nishiyama, and S. Koide, "Electrohydrodynamic drying characteristics of wheat using high voltage electrostatic field," *J. Food Eng.*, vol. 62, no. 3, pp. 209–213, May 2004.

[106] F.-D. Li, L.-T. Li, J.-F. Sun, and E. Tatsumi, "Effect of electrohydrodynamic (EHD) technique on drying process and appearance of okara cake," *J. Food Eng.*, vol. 77, no. 2, pp. 275–280, Nov. 2006.

[107] T. I. Goodenough, P. W. Goodenough, and S. M. Goodenough, "The efficiency of corona wind drying and its application to the food industry," *J. Food Eng.*, vol. 80, no. 4, pp. 1233–1238, Jun. 2007.

[108] T. R. Bajgai and F. Hashinaga, "High electric field drying of Japanese radish," *Dry. Technol.*, vol. 19, no. 9, pp. 2291–2302, Sep. 2001.

[109] A. Esehaghbeygi and M. Basiry, "Electrohydrodynamic (EHD) drying of tomato slices (*Lycopersicon esculentum*)," *J. Food Eng.*, vol. 104, no. 4, pp. 628–631, Jun. 2011.

[110] A. A. Alemrajabi, F. Rezaee, M. Mirhosseini, and A. Esehaghbeygi, "Comparative evaluation of the effects of electrohydrodynamic, oven, and ambient air on carrot cylindrical slices during drying process," *Dry. Technol.*, vol. 30, no. 1, pp. 88–96, Jan. 2012.

[111] S. Isobe, N. Barthakur, T. Yoshino, L. Okushima, and S. Sase, "Electrohydrodynamic drying characteristics of agar gel," *Food Sci. Technol. Res.*, vol. 5, no. 2, pp. 132–136, 1999.

[112] M. Basiry and A. Esehaghbeygi, "Electrohydrodynamic (EHD) drying of rapeseed (*Brassica napus L.*)," *J. Electrostat.*, vol. 68, no. 4, pp. 360–363, Aug. 2010.

[113] F. Lai and K.-W. Lai, "EHD-enhanced drying with wire electrode," *Dry. Technol.*, vol. 20, no. 7, pp. 1393–1405, Jul. 2002.

[114] F. Lai and R. Sharma, "EHD-enhanced drying with multiple needle electrode," *J. Electrostat.*, vol. 63, no. 3, pp. 223–237, Mar. 2005.

[115] Y. Bai, Y. Hu, X. Li, and J. Li, "Experiment study of electrohydrodynamic (EHD) drying scallop," in *Proc. IEEE APPEEC*, Mar. 2009, pp. 1–4.

[116] F. Lai, "A prototype of EHD-enhanced drying system," *J. Electrostat.*, vol. 68, no. 1, pp. 101–104, Feb. 2010.

[117] M. Robinson, *Movement of Air in the Electric Wind of the Corona Discharge*. Somerville, NJ, USA: Hamon Research-Cottrell, 1960.

[118] O. M. Stuetzer, "Ion drag pumps," *J. Appl. Phys.*, vol. 31, no. 1, pp. 136–146, 1960.

[119] E. Moreau and G. Touchard, "Enhancing the mechanical efficiency of electric wind in corona discharges," *J. Electrostat.*, vol. 66, nos. 1–2, pp. 39–44, Jan. 2008.

[120] M. S. June, J. Kribs, and K. M. Lyons, "Measuring efficiency of positive and negative ionic wind devices for comparison to fans and blowers," *J. Electrostat.*, vol. 69, no. 4, pp. 345–350, Aug. 2011.

[121] J.-D. Moon, D.-H. Hwang, and S.-T. Geum, "An EHD gas pump utilizing a ring/needle electrode," *IEEE Trans. Dielectr. Electr. Insul.*, vol. 16, no. 2, pp. 352–358, Apr. 2009.

[122] C. Kim, D. Park, K. C. Noh, and J. Hwang, "Velocity and energy conversion efficiency characteristics of ionic wind generator in a multistage configuration," *J. Electrostat.*, vol. 68, pp. 36–41, Feb. 2009.

[123] H. Bondar and F. Bastien, "Effect of neutral fluid velocity on direct conversion from electrical to fluid kinetic energy in an electro-fluid-dynamics (EFD) device," *J. Phys. D, Appl. Phys.*, vol. 19, no. 9, pp. 1657–1663, Sep. 1986.

[124] K. Asano and K. Yatsuzuka, "Fundamental study of EHD pump with needle-cylinder electrodes," in *Proc. Annu. Rep. Conf. Electr. Insul. Dielectr. Phenomena*, 1999, pp. 785–788.

[125] M. Rickard, D. Dunn-Rankin, F. Weinberg, and F. Carleton, "Characterization of ionic wind velocity," *J. Electrostat.*, vol. 63, no. 6, pp. 711–716, Jun. 2005.

[126] M. Rickard, D. Dunn-Rankin, F. Weinberg, and F. Carleton, "Maximizing ion-driven gas flows," *J. Electrostatics*, vol. 64, no. 6, pp. 368–376, Jun. 2006.

[127] J.-D. Moon, J.-S. Jung, J.-G. Kim, and S.-T. Geum, "An EHD gas pump utilizing a wet porous point electrode," *IEEE Trans. Dielectr. Electr. Insul.*, vol. 16, no. 3, pp. 622–628, Jun. 2009.

[128] H. Nakamura and R. Ohyama, "An image analysis of positive ionic wind velocity under the DC corona discharge in needle-cylinder electrode system," in *Proc. IEEE CEIDP*, Virginia Beach, VA, USA, Oct. 2009, pp. 192–195.

[129] W. Qiu, L. Xia, X. Tan, and L. Yang, "The velocity characteristics of a serial-staged EHD gas pump in air," *IEEE Trans. Plasma Sci.*, vol. 38, no. 10, pp. 2848–2853, Oct. 2010.

[130] Q. Wei, X. Lingzhi, Y. Lanjun, Z. Qiaogen, X. Lei, and C. Li, "Experimental study on the velocity and efficiency characteristics of a serial staged needle array-mesh type EHD gas pump," *Plasma Sci. Technol.*, vol. 13, no. 6, pp. 693–697, Dec. 2011.

[131] L. Zhao and K. Adamiak, "EHD flow in air produced by electric corona discharge in pin-plate configuration," *J. Electrostatics*, vol. 63, nos. 3–4, pp. 337–350, Mar. 2004.

[132] Y. Kitahara, K. Aoyagi, and R. Ohyama, "An experimental analysis of ionic wind velocity characteristics in a needle-plate electrode system by means of laser-induced phosphorescence," in *Proc. IEEE CEIDP*, Vancouver, BC, Canada, Oct. 2007, pp. 529–532.

[133] E. Karakas, A. Begum, and M. Laroussi, "A positive corona-based ion wind generator," *IEEE Trans. Plasma Sci.*, vol. 36, no. 4, pp. 950–951, Aug. 2008.

[134] Y. Otsubo and K. Edamura, "Viscoelasticity of a dielectric fluid in nonuniform electric fields generated by electrodes with flocked fabrics," *Rheol. Acta*, vol. 37, no. 5, pp. 500–507, Nov. 1998.

[135] J. Zhang and F. Lai, "Effect of emitting electrode number on the performance of EHD gas pump in a rectangular channel," *J. Electrostatics*, vol. 69, no. 6, pp. 486–493, Dec. 2011.

[136] P. Magnier, D. Hong, A. Leroy-Chesneau, J.-M. Pouvesle, and J. Hureau, "A DC corona discharge on a flat plate to induce air movement," *J. Electrostatics*, vol. 65, nos. 10–11, pp. 655–659, Oct. 2007.

[137] B. Komeili, J. Chang, G. Harvel, C. Ching, and D. Brocilo, "Flow characteristics of wire-rod type electrohydrodynamic gas pump under negative corona operations," *J. Electrostatics*, vol. 66, no. 5, pp. 342–353, May 2008.

[138] N. Takeuchi and K. Yasuoka, "Efficiency of a wire-rod type electrohydrodynamic gas pump under negative corona operation," *IEEE Trans. Plasma Sci.*, vol. 37, no. 6, pp. 1021–1026, Jun. 2009.

[139] J.-D. Moon, D.-H. Hwang, J.-S. Jung, J.-G. Kim, and S.-T. Geum, "A sliding discharge-type EHD gas pump utilizing a saw-toothed-plate discharge electrode," *IEEE Trans. Dielectr. Electr. Insul.*, vol. 17, no. 3, pp. 742–747, Jun. 2010.

[140] R. Mestiri, R. Hadaji, and S. B. Nasrallah, "An experimental study of a plasma actuator in absence of free airflow: Ionic wind velocity profile," *Phys. Plasmas*, vol. 17, no. 8, pp. 083503-1–083503-7, Aug. 2010.

[141] D. F. Colas, A. Ferret, D. Z. Pai, D. A. Lacoste, and C. O. Laux, "Ionic wind generation by a wire-cylinder-plate corona discharge in air at atmospheric pressure," *J. Appl. Phys.*, vol. 108, no. 10, pp. 103306-1–103306-6, Nov. 2010.

[142] B. Owsenek, J. Seyed-Yagoobi, and R. Page, "Experimental investigation of corona wind heat transfer enhancement with a heated horizontal flat plate," *J. Heat Transf.*, vol. 117, no. 2, pp. 309–315, May 1995.

[143] H. Kalman and E. Sher, "Enhancement of heat transfer by means of a corona wind created by a wire electrode and confined wings assembly," *Appl. Thermal Eng.*, vol. 21, no. 3, pp. 265–282, Feb. 2001.

[144] A. Shooshtari, M. Ohadi, and F. H. R. Franca, "Experimental and numerical analysis of electrohydrodynamic enhancement of heat transfer in air laminar channel flow," in *Proc. 19th Annu. IEEE Semicond. Thermal Meas. Manag. Symp.*, Mar. 2003, pp. 48–52.

[145] L. Zhao, K. Adamiak, and M. Mazumder, "Numerical and experimental studies of the electrohydrodynamic pump for sampling system on Mars," in *Proc. 14th ESA Annu. Meeting Electrostat.*, Minneapolis, MN, USA, Jun. 2008, pp. 683–691.

[146] S. F. Bart, L. S. Tavrow, M. Mehregany, and J. H. Lang, "Microfabricated electrohydrodynamic pumps," *Sens. Actuators A, Phys.*, vol. 21, nos. 1–3, pp. 193–197, Feb. 1990.

[147] A. Richter and H. Sandmaier, "An electrohydrodynamic micropump," in *Proc. Invest. Micro Struct., Sensors, Actuat., Mach. Robots Micro Electro Mech. Syst.*, Napa Valley, CA, USA, Feb. 1990, pp. 99–104.

[148] M. Sen, D. Wajerski, and M. Gad-el-Hak, "A novel pump for MEMS applications," *Trans. ASME J. Fluids Eng.*, vol. 118, no. 3, pp. 624–627, 1996.

[149] J. M. Crowley, G. S. Wright, and J. C. Chato, "Selecting a working fluid to increase the efficiency and flow rate of an EHD pump," *IEEE Trans. Ind. Appl.*, vol. 26, no. 1, pp. 42–49, Feb. 1990.

[150] A. H. Sharbaugh and G. W. Walker, "The design and evaluation of an ion-drag dielectric pump to enhance cooling in a small oil-filled transformer," *IEEE Trans. Ind. Appl.*, vol. 21, no. 4, pp. 950–955, Jul. 1985.

[151] M. Bologa, I. Kozhevnikov, and I. Kozhukhari, "Multistage electrohydrodynamical pump," in *Proc. Annu. Rep. Conf. IEEE Electr. Insul. Dielectr. Phenomena*, vol. 1. Victoria, BC, Canada, Oct. 2000, pp. 57–60.

[152] I. Kojevnikov, O. Motorin, M. Bologa, and A. Kojevnikova, "Optimization of the electrohydrodynamic pump," in *Proc. Annu. Rep. Conf. IEEE Electr. Insul. Dielectr. Phenomena*, Aug. 2002, pp. 204–207.

[153] I. Kano, K. Mizuochi, and I. Takahashi, "Micro-electrohydrodynamic pump by dielectric fluid: Improvement for performance of pressure using cylindrical electrodes," in *Proc. 6th JFPS Int.*, vol. 2. 2005, pp. 1–3.

[154] I. Kano and I. Takahashi, "Improvement for pressure performance of micro-EHD pump with an arrangement of thin cylindrical electrodes," *Jsme Int. J. Series B, Fluids Thermal Eng.*, vol. 49, no. 3, pp. 748–754, Jan. 2006.

[155] G. Fuhr, R. Hagedorn, T. Muller, W. Benecke, and B. Wagner, "Microfabricated electrohydrodynamic (EHD) pumps for liquids of higher conductivity," *Microelectromech. Syst.*, vol. 1, no. 3, pp. 141–146, Sep. 1992.

[156] G. Fuhr, R. Hagedorn, T. Muller, W. Benecke, and B. Wagner, "Pumping of water solutions in microfabricated electrohydrodynamic systems," in *Proc. IEEE Invest. Micro Struct., Sensors, Actuat., Mach. Robots Micro Electro Mech. Syst.*, Feb. 1992, pp. 25–30.

[157] Y. Zhao, P. Foroughi, J. Lawler, and M. Ohadi, "Development of an electrohydrodynamic (EHD) micro pump for LN2 spot cooling," in *Proc. Int. Mech. Eng. Congr. Exposit.*, Washington, DC, USA, Nov. 2003, pp. 113–118.

[158] P. Foroughi, V. Benetis, M. Ohadi, Y. Zhao, and J. Lawler, "Design, testing and optimization of a micropump for cryogenic spot cooling applications," in *Proc. IEEE 21st Annu. Semicond. Thermal Meas. Manag. Symp.*, Mar. 2005, pp. 335–340.

[159] C. C. Wong, D. R. Adkins, and D. Chu, "Development of a micropump for microelectronic cooling," in *Proc. Int. Mech. Eng. Congr. Exhibit.*, Atlanta, GA, USA, 1996, pp. 1–6.

[160] A. Si-Hong and K. Yong-Kweon, "Fabrication and experiment of planar micro ion drag pump," in *Proc. Int. Conf. Solid State Sensors Actuat.*, vol. 1. Chicago, IL, USA, Jun. 1997, pp. 373–376.

[161] J. Darabi, M. M. Ohadi, and D. DeVoe, "An electrohydrodynamic polarization micropump for electronic cooling," *J. Microelectromech. Syst.*, vol. 10, no. 1, pp. 98–106, Mar. 2001.

[162] J. Darabi, M. Rada, M. Ohadi, and J. Lawler, "Design, fabrication, and testing of an electrohydrodynamic ion-drag micropump," *J. Microelectromech. Syst.*, vol. 11, no. 6, pp. 684–690, Dec. 2002.

[163] S. Chowdhury, J. Darabi, M. Ohadi, and J. Lawler, "Chip integrated micro cooling system for high heat flux electronic cooling applications," in *Proc. Int. Conf. Thermal Challenges Next Generat. Electron. Syst.*, 2002, pp. 85–93.

[164] J. Darabi and K. Ekula, "Development of a chip-integrated micro cooling device," *Microelectron. J.*, vol. 34, no. 11, pp. 1067–1074, Nov. 2003.

[165] V. Benetis, A. Shooshtari, P. Foroughi, and M. M. Ohadi, "A source-integrated micropump for cooling of high heat flux electronics," in *Proc. 19th Annu. IEEE Semicond. Thermal Meas. Manag. Symp.*, Mar. 2003, pp. 236–241.

[166] C. K. Lee, A. J. Robinson, and C. Y. Ching, "Development of EHD ion-drag micropump for microscale electronics cooling," in *Proc. 13th Int. Workshop Thermal Invest. ICs Syst.*, Sep. 2007, pp. 1–6.

[167] H. Yu, J. Yu, and C. Ma, "Design, fabrication and experimental research for an electrohydrodynamic micropump," *Sci. China Technol. Sci.*, vol. 53, no. 10, pp. 2839–2845, Oct. 2010.

[168] J. Darabi and C. Rhodes, "CFD modeling of an ion-drag micropump," *Sens. Actuators A, Phys.*, vol. 127, no. 1, pp. 94–103, Feb. 2006.

[169] A. Rashkovan, E. Sher, and H. Kalman, "Experimental optimization of an electric blower by corona wind," *Appl. Thermal Eng.*, vol. 22, no. 14, pp. 1587–1599, Oct. 2002.

[170] F. Yang, N. E. Jewell-Larsen, D. L. Brown, K. Pendergrass, D. A. Parker, I. A. Krichtafovitch, *et al.*, "Corona driven air propulsion for cooling of electronics," in *Proc. 13th Int. Symp. High Volt. Eng.*, Rotterdam, The Netherlands, 2003, pp. 1–4.

[171] N. E. Jewell-Larsen, E. Tran, I. A. Krichtafovitch, and A. V. Mamishev, "Design and optimization of electrostatic fluid accelerators," *IEEE Trans. Dielectr. Electr. Insul.*, vol. 13, no. 1, pp. 191–203, Feb. 2006.

[172] D. Schlitz and V. Singhal, "An electro-aerodynamic solid-state fan and cooling system," in *Proc. 34th Annu. IEEE Semicond. Thermal Meas. Manag. Symp.*, Mar. 2008, pp. 46–49.

[173] N. E. Jewell-Larsen, H. Ran, Y. Zhang, M. K. Schwiebert, K. A. H. Tessera, and A. V. Mamishev, "Electrohydrodynamic (EHD) cooled laptop," in *Proc. 25th Annu. IEEE Semicond. Thermal Meas. Manag. Symp.*, Mar. 2009, pp. 261–266.

[174] N. Jewell-Larsen, Y. Zhang, M. Schwiebert, and K. Honer, "Collector-radiator structure for an electrohydrodynicamic cooling system," U.S. Patent 072 036, Jun. 16, 2011.

[175] N. Jewell-Larsen, K. Honer, and G. Joseph, "Electronic system adapted for passive convective cooling and staged use of electrohydrodynamic (EHD) and mechanical air movers for quiet forced convection assist," U.S. Patent 0 205 079, Aug. 16, 2012.
[176] N. Jewell-Larsen, "Electrohydrodynamic (EHD) fluid mover with field shaping feature at leading edge of collector electrodes," U.S. Patent 145 698, Oct. 26, 2012.
[177] J.-S. Chang, H. Tsubone, G. Harvel, and K. Urashima, "Capillary/narrow flow channel driven EHD gas pump for an advanced thermal management of micro-electronics," in *Proc. IEEE IAS Annu. Meeting*, Oct. 2008, pp. 1–8.
[178] J.-S. Chang, H. Tsubone, G. D. Harvel, and K. Urashima, "Narrow-flow-channel-driven EHD gas pump for an advanced thermal management of microelectronics," *IEEE Trans. Ind. Appl.*, vol. 46, no. 3, pp. 1151–1158, Jun. 2010.
[179] A. O. Ong, A. R. Abramson, and N. C. Tien, "Optimized and microfabricated ionic wind pump array as a next generation solution for electronics cooling systems," in *Proc. 13th IEEE Intersoc. Conf. Thermal Thermomech. Phenomena Electron. Syst.*, San Diego, CA, USA, May 2012, pp. 1306–1311.
[180] I. Y. Chen, M.-Z. Guo, K.-S. Yang, and C.-C. Wang, "Enhanced cooling for LED lighting using ionic wind," *Int. J. Heat Mass Transf.*, vol. 57, no. 1, pp. 285–291, Jan. 2013.
[181] N. E. Jewell-Larsen, S. V. Karpov, H. Ran, P. Savalia, and K. A. Honer, "Investigation of dust in electrohydrodynamic (EHD) systems," in *Proc. 26th Annu. IEEE Semicond. Thermal Meas. Manag. Symp.*, Santa Clara, CA, USA, Feb. 2010, pp. 249–255.
[182] J. Podlinski, A. Niewulis, A. Berendt, and J. Mizeraczyk, "Pumping effect measured by PIV method in multi-layer spike electrode EHD device for air cleaning," *IEEE Trans. Ind. Appl.*, vol. 49, no. 6, pp. 2402–2408, Dec. 2013.

Emmanouil D. Fylladitakis received the B.Sc. degree in electrical energy engineering from the Technological Educational Institute (TEI) of Athens, Athens, Greece, and the M.Sc. (Hons.) degree in energy from Heriot-Watt University, Edinburgh, Scotland, in 2010 and 2012, respectively. He is currently pursuing the Ph.D. degree with the Electronics and Computer Engineering Department, Brunel University London, London, U.K.

He is currently an External Research Associate with the TEI of Athens. His current research interests include corona discharges, electrohydrodynamic effects, renewable energy systems, energy conservation in buildings, engineering education, and distance learning systems.

Mr. Fylladitakis received a prize for outstanding merit from Heriot-Watt University.

Michael P. Theodoridis received the B.Sc. degree in energy engineering from the Technological Educational Institute (TEI) of Athens, Athens, Greece, the M.Sc. degree in power electronics and drives jointly from the University of Birmingham, Birmingham, U.K., and the University of Nottingham, Nottingham, U.K., and the Ph.D. degree in electrical engineering from the University of Birmingham in 2000, 2002, and 2005, respectively.

He was with Olympic Airways, Athens, from 2000 to 2001. From 2005 to 2011, he was with the Department of Energy Technology Engineering, TEI of Athens. He currently is with Brunel University London, London, U.K. His main research interest is high-frequency power conversion.

Antonios X. Moronis was born in Athens, Greece, in 1967. He received the Diploma degree in electrical engineering from the Aristotle University of Thessaloniki, Thessaloniki, Greece, and the Ph.D. degree in electrical engineering from the National Technical University of Athens, Athens, Greece, in 1990 and 1995, respectively.

He was an Assistant Professor with the Energy Engineering Department, Technological Educational Institute, Athens, from 2001 to 2006. He is currently an Associate Professor with the same department and the Director of the Electrotechnology and Measuring Systems Laboratory. He has authored more than 45 articles in scientific journals and conference proceedings. His current research interests include dielectrics and electrical insulation, electrohydrodynamics, high voltage applications, earthing systems in electrical installations and fault diagnosis, and predictive maintenance of electric power system components.

Dr. Moronis is a member of the Technical Chamber of Greece.